

# 1 Formation of Mega-Scale Glacial Lineations on the Dubawnt Lake Ice 2 Stream Bed: 1. Size, Shape and Spacing from a Large Remote Sensing

## 3 Dataset

4 <sup>1</sup>Stokes, C.R., <sup>2</sup>Spagnolo, M., <sup>3</sup>Clark, C.D., <sup>1</sup>O’Cofaigh, C., <sup>4</sup>Lian, O.B. and <sup>1</sup>Dunstone, R.B.

5  
6 <sup>1</sup>*Department of Geography, Durham University, Durham DH1 3LE, UK (c.r.stokes@durham.ac.uk)*

7 <sup>2</sup>*School of Geosciences, University of Aberdeen, UK*

8 <sup>3</sup>*Department of Geography, University of Sheffield, UK*

9 <sup>4</sup>*Department of Geography, University of the Fraser Valley, Abbotsford, B.C., Canada*

### 10 11 12 **Abstract:**

13 Mega-scale glacial lineations (MSGs) are the largest flow parallel bedforms produced by ice  
14 sheets and are formed beneath rapidly-flowing ice streams. Knowledge of their characteristics  
15 and genesis is likely to result in an improved understanding of the rate at which ice and  
16 sediment are discharged by ice sheets, but there is little consensus as to how they are formed  
17 and there are few quantitative datasets of their characteristics with which to formulate or test  
18 hypotheses. This paper presents the results of a remote sensing survey of ~46,000 bedforms  
19 on the Dubawnt Lake palaeo-ice stream bed, focussing on a central transect of 17,038 that  
20 includes highly elongate bedforms previously described as MSGs. Within this transect,  
21 lineations exceed 10 km in length (max. >20 km) and 23% have elongation ratios >10:1  
22 (max. 149:1). Highly elongate features are interspersed with much shorter drumlin-like  
23 features, but longer bedforms are typically narrower, suggesting that their length develops  
24 more quickly than, or at the expense of, their width. Bedforms are broadly symmetrical in  
25 plan-form and have a preferred lateral spacing of 50–250 m, which implies a regular, rather

26 than random, pattern of corrugations. Comparison with drumlins reveals that the more  
27 attenuated MSGs simply extend the ‘tail’ of the distribution of data, rather than plotting as a  
28 separate population. Taken together, this supports the idea of a subglacial bedform continuum  
29 primarily controlled by ice velocity, but existing hypotheses of MSG formation are either  
30 not supported, or are insufficiently developed to explain our observations. Rather, we  
31 conclude that, under conditions of rapid ice flow, MSGs attain their great length relatively  
32 quickly (decades) through a probable combination of subglacial deformation, which  
33 attenuates ridges, and erosional processes that removes material from between them.

34

35

## 36 **1. Introduction**

37 Mega-scale glacial lineations (MSGs) are highly elongate ridges of sediment produced  
38 subglacially (Clark, 1993). They are similar to other flow parallel bedforms (e.g. flutes and  
39 drumlins) but are typically much longer (~10–100 km), wider (ca. 200–1300 m); and have  
40 lateral wavelengths (spacing) of 0.2–5 km and amplitudes from just a few metres to several  
41 10s of metres (Clark, 1993; Clark *et al.*, 2003). Although observations of large and highly  
42 elongate glacial bedforms have been noted for several decades (e.g. Tyrell, 1906; Dean,  
43 1953; Lemke, 1958), they were not formally recognised and named until the early 1990s (see  
44 Clark, 1993), following the advent of satellite imagery that enabled a large-scale view of  
45 palaeo-ice sheet beds. Although they are commonly identified and mapped as ridges, some  
46 workers have taken the view that, collectively, their appearance is more akin to a grooved or  
47 corrugated till surface (e.g. Dean, 1953; Lemke, 1958; Heidenreich, 1964; Clark *et al.*, 2003;  
48 Stokes & Clark, 2003a). In this paper, we refer to MSG in their broadest sense and include  
49 features that are variously described as ‘bundle structures’ (Canals *et al.*, 2000), ‘mega-  
50 flutings’ (e.g. Shaw *et al.*, 2000), ‘megalineations’ (Shaw *et al.*, 2008), and ‘megagrooves’

51 (Bradwell *et al.*, 2008), all of which fit the characteristics of MSGL described in Clark  
52 (1993).

53 Determining the origin of MSGLs represents a key scientific challenge and various  
54 hypotheses have been put forward and include subglacial sediment deformation (Clark,  
55 1993), catastrophic meltwater floods (Shaw *et al.*, 2000; 2008), groove-ploughing (Clark *et*  
56 *al.*, 2003), spiral flows in basal ice (Schoof and Clarke, 2008), and a rilling instability in  
57 subglacial meltwater flow (Fowler, 2010). Although there is little agreement about the  
58 genesis of MSGLs, a key aspect of their formation is their association with areas of rapidly-  
59 flowing ice (King *et al.*, 2009). Clark (1993) was the first to suggest that their great length  
60 might be related to rapid ice flow and later work has confirmed the notion that bedform  
61 attenuation is related to ice velocity (cf. Hart, 1999; Ó Cofaigh *et al.*, 2002; Stokes and Clark,  
62 2002; Briner, 2007). Indeed, the presence of MSGLs has been used to infer the location of  
63 numerous palaeo-ice streams (cf. Stokes and Clark, 1999; Canals *et al.*, 2000; Ó Cofaigh *et*  
64 *al.*, 2002, 2010; Stokes and Clark, 2003a; b; Graham *et al.*, 2009; Livingstone *et al.*, 2012)  
65 including immediately down-ice from existing ice streams (cf. Shipp *et al.*, 1999; Wellner *et*  
66 *al.*, 2006) and, most recently, beneath active ice streams (cf. King *et al.*, 2009; Jezek *et al.*,  
67 2011).

68 Given the importance of ice streams to ice sheet mass balance and concerns over their recent  
69 and future dynamics (e.g. Pritchard *et al.*, 2009), it is becoming increasingly important to  
70 understand the subglacial processes that facilitate their flow and govern the rate at which both  
71 ice and sediment are discharged by ice sheets. Moreover, because we now know that MSGL  
72 are one manifestation of these processes, a better understanding of the mechanism by which  
73 they form is likely to result in a major advance in our knowledge of the basal processes that  
74 act to sustain or inhibit ice stream flow. To date, however, most accounts of MSGLs are  
75 restricted to qualitative descriptions of their characteristics and, compared to drumlins (e.g.

76 Clark *et al.*, 2009; Hess and Briner, 2009; Spagnolo *et al.*, 2010, 2011, 2012; Stokes *et al.*,  
77 2011), there are few systematic measurement of their dimensions and morphometry based on  
78 large sample sizes (e.g. Graham *et al.*, 2009) and few observations of their sedimentology and  
79 stratigraphy (e.g. Lemke, 1958; Shaw *et al.*, 2000).

80 To address these issues, we have undertaken a multi-scaled mapping and field campaign to  
81 characterise the size, shape, spacing, and composition of MSGs on the bed of the previously  
82 identified Dubawnt Lake palaeo-ice stream (Stokes and Clark, 2003b), which operated in a  
83 part of the Laurentide Ice Sheet (LIS). This ice stream was selected because it contains tens  
84 of thousands of bedforms and represents a pristine landscape formed by a late and relatively  
85 brief episode of ice streaming, with very limited over-printing by younger events (Stokes and  
86 Clark, 2003b). Our results are reported in two papers that focus on: (1) their morphometry  
87 and pattern from remote sensing (Paper 1), and (2), their sedimentology and stratigraphy  
88 from sediment exposures (Paper 2: Ó Cofaigh *et al.*, submitted). The aim of this paper is to  
89 provide a substantive dataset (several thousand bedforms) on the size, shape and pattern of  
90 MSGs. Our focus is on reporting a statistically robust population to ascertain their key  
91 characteristics (cf. Clark *et al.*, 2009) and assess the implications for their formation. For  
92 example, what is their typical size and shape, how are they grouped, and how might this be  
93 related to ideas of their formation? To what extent might they be related to drumlins, e.g. do  
94 they form part of a glacier bedform continuum (Rose, 1987) or are they, in this sense, discrete  
95 landforms?

96

97

## 98 **2. Previous work on the Dubawnt Lake palaeo-ice stream**

99 The Dubawnt Lake Ice Stream (DLIS) bed is located on the north-western Canadian Shield  
100 and spans the border between Nunavut and Northwest territories, see Figure 1. Tyrrell (1906)

101 was the first to describe the ‘drumlinoid’ ridges that characterise the region known as the  
102 Barren Grounds and early work in this area noted the highly elongate glacial lineations north-  
103 west of Dubawnt Lake (e.g. Bird, 1953; Craig, 1964), which Dean (1953: p. 21) described as  
104 having a “longitudinal axis 15 to 30 times the length of the transverse axis”. More recently,  
105 Aylsworth and Shilts (1989a) speculated about the possible role of rapid ice flow in creating  
106 the spectacular flutings and the distinctive ‘bottle-neck’ flow pattern that is clearly  
107 identifiable on the Glacial Map of Canada (Prest *et al.*, 1968). This distinct bedform pattern  
108 was also mapped by Boulton and Clark (1990), who attributed its formation to a late glacial  
109 event in their reconstruction of the LIS. This interpretation was later supported by Kleman  
110 and Borgström (1996), who used the Dubawnt Lake flow-set as an exemplar of a ‘surge fan’  
111 in their glacial inversion model for reconstructing palaeo-ice sheets. Surge fans are thought to  
112 form during the decay stages of an ice sheet, often in relation to proglacial lake basins, and  
113 lineations are thought to form nearly synchronously over the whole fan area (Kleman and  
114 Borgström, 1996).

115 Building on this work, Stokes and Clark (2003b) used remote sensing techniques to undertake  
116 a detailed analysis of the ice stream bed and confirmed that the flow-set was formed by a  
117 palaeo-ice stream that operated for a few hundred years during deglaciation, just prior to 8.2  
118 <sup>14</sup>C ka BP. Stokes and Clark (2003c) highlighted the unusual location of the ice stream on the  
119 relatively hard bedrock of the Canadian Shield, although parts of the ice stream are underlain  
120 by softer sedimentary rocks, including the extensive sandstones of the Thelon sedimentary  
121 basin, which underlies the most elongate bedforms. The ice stream is thought to have been  
122 triggered by the development of a proglacial lake which induced high calving rates and  
123 drawdown of ice from points further inland (Stokes and Clark, 2004). Indeed, ice stream  
124 activity and the associated thinning of the ice sheet was probably responsible for the final  
125 south-eastward migration of the Keewatin Ice Divide and the subsequent deglaciation of the

126 area (McMartin and Henderson, 2004). It has also been noted that parts of the ice stream bed  
127 (~7%) are characterised by ribbed moraines that are superimposed on the elongate bedforms  
128 produced by the ice stream (e.g. Aylsworth and Shilts, 1989a; Stokes *et al.*, 2006). Stokes *et*  
129 *al.* (2008) suggested that these ribbed moraines were generated during ice stream shut-down  
130 when the till stiffened as a result of dewatering and/or basal freeze-on (cf. Christofferson and  
131 Tulaczyk, 2003). Apart from the ribbed moraines, no other (younger) ice flow events are  
132 superimposed on the flow-set and, because it represents a coherent bedform pattern with  
133 individual lineations displaying exceptional parallel conformity to neighbouring bedforms, it  
134 can be assumed that they are all related to the flow and final stoppage of the ice stream (cf.  
135 Stokes and Clark, 2003b; 2008).

136 In terms of its dimensions, the ice stream is reconstructed at ~450 km in length and it depicts  
137 a broad zone of flow convergence into a narrower main ‘trunk’ (~140 km wide), which then  
138 diverges towards a lobate terminus (cf. Stokes and Clark, 2003b) (Fig. 1). Mapping of  
139 selected along-flow transects of glacial lineations revealed that their elongation ratio matches  
140 the expected pattern of ice velocity across the flow-set (Stokes and Clark, 2002; 2003b). The  
141 longest lineations (>10 km in length) occur in the main ‘trunk’ of the ice stream where  
142 elongation ratios have been reported to approach 50:1 (Stokes and Clark, 2003b), clearly  
143 placing them in the category of MSGLs (cf. Clark, 1993).

144

145

### 146 **3. Methods**

#### 147 *3.1. Data sources and mapping*

148 We compiled complete coverage of the ice stream bed (and surroundings) with cloud-free  
149 scenes from the Landsat Enhanced Thematic Mapper Plus satellite, downloaded from the  
150 Global Land Cover Facility (<http://glcf.umiacs.umd.edu/>). This imagery is orthorectified with

151 a multispectral spatial resolution of 30 m (bands 1-5, 7; band 6 = 60 m), 15 m in  
152 panchromatic (band 8). This resolution has been shown to be more than sufficient for the  
153 mapping of large-scale glacial geomorphology, e.g. drumlins, ribbed moraines, major  
154 terminal moraines, etc. (cf. Clark, 1997). In addition, we also acquired around 300  
155 panchromatic aerial photographs (hard copy) from the Canadian National Air Photo library in  
156 Ottawa.

157 Previous work mapped 8,856 lineations from transects along the southern half of the ice  
158 stream bed (Stokes and Clark, 2002; 2003). We use these data and supplement them with new  
159 mapping of every lineation on the entire ice stream bed (flow-set), irrespective of its location  
160 or dimensions, i.e. we used no preconceived definition of MSGs to select the ones that we  
161 would map. Given that the flow-set contains tens of thousands of bedforms, each lineation  
162 was simply depicted with a single line along the ridge crest. These data provide a simple  
163 measure of bedform length and location, which is useful for calculating derivatives such as  
164 wavelengths (spacing), density, pattern and orientation. However, our specific aim was to  
165 collate a large sample of data that also included the width and shape of MSGs that are  
166 known to exist in the narrowest part of the flow-set (cf. Stokes and Clark, 2002; 2003b). This  
167 was achieved by mapping a broad transect of lineations from the central trunk of the ice  
168 stream (where the longest bedforms occur) and digitising around their break-of-slope as  
169 polygon features (e.g. Clark *et al.*, 2009). Figure 2 shows the coverage of satellite imagery,  
170 the extent of the ice stream flow-set (mapped as lines), and the extent of the DLIS transect  
171 mapped as polygons, along with examples of some mapped lineations.

172 Mapping using satellite imagery was cross-checked using aerial photographs taken of specific  
173 regions (e.g. Stokes *et al.*, 2006) and ground-truthing was undertaken for specific areas  
174 during fieldwork in the summers of 2004, 2005 and 2006. Ideally, we would have liked to  
175 have obtained data on lineation height (e.g. Spagnolo *et al.*, 2012) but, given the low

176 amplitude of most of the features (~5 m), this would have required elevation data (e.g. a  
177 Digital Elevation Model) with a spatial resolution of just a few metres, which is not presently  
178 available for this region.

179

### 180 3.2. Measurement of lineation size

181 For lineations mapped as a single line (from hereon referred to as the ‘ice stream flowset’  
182 database), we used a Geographical Information System (GIS: ArcMap) to extract the length  
183 ( $L$ ) and location (mid-point ( $M$ ) of each line). For the zone of more elongate bedforms across  
184 the central transect of the ice stream flowset mapped as a polygons (from hereon referred to  
185 as the ‘DLIS transect’), the area ( $A$ ) is extracted from the GIS and, following Spagnolo *et al.*  
186 (2010), the length ( $L$ ) was derived from a tool that plots the longest straight line within the  
187 mapped polygon, see Figure 3a, and this also gives orientation and defines the location of the  
188 upstream ( $U$ ) and down-stream ( $D$ ) limits of the bedform (i.e. the start point and end point of  
189  $L$ ). The width ( $W$ ) is then derived from another tool that extracts the longest straight line  
190 perpendicular to  $L$  (Fig. 3a), which also gives the intersect ( $I$ ). The elongation ratio ( $ER$ ) is  
191 simply the ratio of  $L:W$ .

192

### 193 3.3. Measurement of lineation shape

194 Using the parameters described above, Spagnolo *et al.* (2010) developed simple methods to  
195 explore the planar (plan-form) shape of drumlins in order to test the long-standing idea that  
196 they are asymmetric (i.e. larger, blunter upstream and thinner, tapering downstream: e.g.  
197 Chorley, 1959). Although there are different ways of quantifying the plan-form, we use a  
198 method from Spagnolo *et al.* (2010) that divides the shape of the bedform into an upstream  
199 and downstream half. Each polygon is split in half by a line perpendicular to its length ( $L$ )

200 and passing through midpoint ( $M$ ) of  $L$ . In this way, drumlin planar asymmetry  $As_{pl\_a}$  is  
201 described as:

202

$$203 \quad As_{pl\_a} = (A_{up}/A)$$

204

205 Where  $A_{up}$  = upstream area, and  $A$  = total area (Fig. 3b-d). Higher values indicate upstream  
206 halves that are larger than downstream halves (i.e. classically asymmetric: Fig. 3b) and lower  
207 values indicate downstream halves that are larger than upstream halves (i.e. reversed  
208 asymmetry: Fig. 3d).

209

#### 210 *3.4. Measurement of lineation density and 'packing'*

211 We make distinctions between point density (simply the number of bedforms per unit area),  
212 linear density (the cumulative length of lineation per unit area), and areal density (or  
213 'packing': the cumulative area of lineations per unit area). Thus, point density is simply  
214 extracted from the number of lineations, as recorded by a point location ( $M$ , above) per unit  
215 area (and can be extracted from both the entire flow-set and the DLIS transect); linear density  
216 is extracted from the cumulative length of lineations per unit area (e.g. from the entire flow-  
217 set); whereas packing is extracted from the cumulative surface area of lineations, per unit  
218 area (which can only be extracted from DLIS transect mapped as polygons).

219

#### 220 *3.5. Measurement of lineation spacing*

221 In addition to their density or packing, we also quantify bedform spacing and pattern, which  
222 has only been measured in a handful of studies (e.g. Smalley and Unwin, 1968). Nearest  
223 neighbour analysis of drumlin fields has been shown to be fraught with methodological  
224 deficiencies associated with sampling areas (cf. Clark, 2010) and has led to contradictory

225 results (e.g. Smalley and Unwin, 1968; Baronowksi, 1977; Boots and Burns, 1984). In this  
226 paper, we simplify quantification of bedform spacing to two measurements. The first  
227 calculates the distance to the nearest lineation in the along-flow direction (longitudinal  
228 spacing) and the second calculates the distance to the nearest lineation in the across-flow  
229 direction (transverse/lateral spacing). Although flow-lines within the flow-set are curvilinear,  
230 these distances can be approximated as straight lines because bedforms are packed closely  
231 together.

232 The longitudinal spacing of the mapped lineaments was evaluated using a specific GIS  
233 technique based on three fundamental steps (Spagnolo *et al.*, in prep). Firstly, the direction of  
234 ice flow is derived relative to each individual bedform as the average azimuth of the 10  
235 closest bedforms. The 10 nearest bedforms are identified using the MSGL mid-points (*M*: see  
236 Fig. 3) and using a specific GIS application called ‘distance between points’ in Hawth’s  
237 Analysis Tools, which is an extension for ESRI’s ArcGIS. Second, the closest along-flow  
238 bedform is identified. Given the average azimuth, the longitudinal distances between each  
239 individual MSGL and its 10 neighbours can be evaluated geometrically (by applying the  
240 Pythagorean theorem). The shortest distance is used to identify the closest longitudinal  
241 neighbour. A filter is also applied to guarantee that the identified closest bedform is aligned  
242 with the original bedform. This is done by analyzing the across-flow distance between a  
243 MSGL midpoint and its closest bedform’s midpoint, and by verifying that this does not  
244 exceed half the original MSGL width. Third, the real distance (‘gap’) between each nearest  
245 bedform pair is evaluated by subtracting the half-lengths of the two bedforms from the  
246 absolute distance between their midpoints. The transverse spacing technique follows exactly  
247 the same steps, the only difference being that the shadow is projected transverse  
248 (perpendicular) to the ice flow direction and that the gap distance is obtained by subtracting  
249 the half-widths of the two bedforms from the absolute distance between their mid-points.

250  
251  
252  
253  
254  
255  
256  
257  
258  
259  
260  
261  
262  
263  
264  
265  
266  
267  
268  
269  
270  
271  
272  
273  
274

## **4. Results**

### *4.1. Lineation length and distribution from the ice stream flow-set*

Mapping of the entire ice stream flow-set reveals a total of 42,583 lineations, with each bedform depicted by a single line along its ridge crest, parallel to ice flow. The mean length of bedforms across the entire ice stream flow-set is 879 m (median length = 667 m) and Figure 4a shows their distribution, with each line feature coloured according to its length. As noted in previous work based on more limited mapping (e.g. Stokes and Clark, 2002; 2003b), there is a clear pattern, with the most elongate bedforms occurring in the central, narrower, trunk of the ice stream tract, where velocities are assumed to have been highest. In this zone, lineations commonly exceed 5 km in length and this region is the focus of our more detailed mapping of the features as polygons, where we have mapped a total of 17,038 lineations across a broad transect in the central trunk (see Fig. 2). Figures 4b and 4c show a sample of the mapping of this region, which illustrates numerous bedforms between 5 and ~20 km in length and elongation ratios commonly in excess of 30:1. Figure 5 shows examples of these distinctive bedforms as they appear on satellite imagery and oblique aerial photography.

Histograms of lineation length from both the entire ice stream flow-set and the DLIS transect are shown in Figure 6. Both populations show unimodal distributions with a strong positive skew (very long tail) and whilst it is clear that the DLIS transect is a sub-sample of more elongate bedforms (MSGs), it should be noted that shorter lineations also occur within this region, such that the populations clearly overlap. This is also apparent as small-scale heterogeneity within the general patterns seen in Figure 4.

Our results now focus on the DLIS transect as a means of characterising the size and shape of the most elongate bedforms. Note that we choose to measure the size and shape of *all* of the

275 lineations in the DLIS transect (including smaller features that might be better described as  
276 drumlins), rather than selecting a sub-sample of lineations above a certain size to characterise  
277 the field of MSGLs. Our justification for this is threefold: (i), there is no strict definition or  
278 physical basis to differentiate and select MSGLs from shorter bedforms and so any threshold  
279 (e.g. an elongation ratio >10:1, cf. Stokes & Clark, 1999) would be somewhat arbitrary and  
280 difficult to justify; (ii), the use of any threshold to distinguish MSGLs would introduce  
281 circular arguments, i.e. we select a sub-population of elongate bedforms and then use these to  
282 show that they are more elongate than other bedforms; and (iii), the MSGLs in this particular  
283 flow-set are clearly associated with less elongate bedforms (e.g. Fig. 4) and, given that we  
284 know it represents a single, short-lived episode of ice stream flow (Stokes and Clark, 2003b),  
285 we regard this as an important observation for constraining theories of their formation.

286

#### 287 *4.2. Length, width and elongation ratio of bedforms from the DLIS transect*

288 Histograms of length, width and elongation ratio of the lineations from the DLIS transect are  
289 shown in Figure 7. The mean length is 945 m (min. = 186 m; max. = 20,146 m) and the mean  
290 width is ~117 m (min. = 39; max. = 533), see Table 1. Elongation ratios are particularly  
291 striking, with a mean of 8.7 (min. = 2.2) and with 23% in excess of 10:1. The maximum is  
292 149:1 which is, to our knowledge, the highest ever reported in the literature. All distributions  
293 are unimodal with a strong positive skew, as has been observed for a large population of  
294 drumlins (cf. Clark *et al.*, 2009).

295 Relationships between length, width and elongation ratio (cf. Clark *et al.*, 2009) are plotted in  
296 Figure 8. A plot of length versus width (Fig. 8a) reveals only a weak tendency for longer  
297 bedforms to be wider. A power law function gives a higher  $r^2$  (0.53) than a simple linear  
298 relationship ( $r^2 = 0.24$ ), although neither fit particularly well. Indeed, the very longest  
299 bedforms (e.g. >10 km) tend to be narrower and the widest bedforms tend to be <5 km long.

300 Unsurprisingly, bedform length and elongation ratio (Fig. 8b) are strongly correlated because  
301 elongation ratio is derived from length. Linear and power law functions give similar  $r^2$  values  
302 ( $\sim 0.70$ ), but the fact that these correlations are not even higher indicates that bedforms of a  
303 certain length can exhibit a range of elongation ratios, e.g. lineations 5 km long exhibit  
304 elongation ratios from  $<10:1$  to  $>60:1$ . Shorter bedforms (e.g.  $<5$  km) have a lower range of  
305 elongation ratios, as seen in the tighter clustering of points towards the origin of the  
306 scatterplot. The correlation between width and elongation ratio reveals weak correlations,  
307 with neither a linear ( $r^2 = 0.12$ ) or power law function ( $r^2 = 0.19$ ) providing a good  
308 description of the data. However, the plot clearly shows that bedforms with the highest  
309 elongation ratios (e.g.  $>40:1$ ) tend to be narrower. No bedform with a width  $>400$  m, for  
310 example, attains an elongation ratio  $>20:1$ .

311

#### 312 *4.3 Planar shape of bedforms from the DLIS transect*

313 Measurements of the planar shape ( $As_{pl_a}$ ) of bedforms within the DLIS transect are plotted  
314 as a histogram in Figure 9. The mean and median value for bedforms in the DLIS transect is  
315 0.52, which indicates a very slight tendency towards classical asymmetry (modal class in Fig.  
316 9 is 0.50 to 0.52 and 19% of bedforms fall within this class: Table 1). The data are tightly  
317 clustered (5<sup>th</sup> percentile = 0.45; 95<sup>th</sup> percentile is 0.59) but there are extreme cases of  
318 bedforms that are clearly asymmetric in the classic sense (max = 0.73) and in the reverse  
319 sense (min = 0.31), i.e. with downstream halves much larger than their upstream halves.

320 Figure 10 plots the planar shape across the entire transect and indicates that there are no  
321 obvious clusters where large numbers of bedforms ( $n > 10$ ) exhibit a preferred preference for  
322 classic or reverse asymmetry. However, there are some places where small groups of  
323 bedforms ( $\sim 5-10$ ) that are classically asymmetric sit alongside each other (Fig. 10b). There  
324 are no similar patches for those that show reverse asymmetry.

325

#### 326 *4.4. Patterning and spacing of MSGL*

327 The density of lineations across the entire flow-set is shown in Figure 11 as both number of  
328 lineations per unit area (Fig. 11a) and cumulative length of lineations per unit area (Fig. 11b).  
329 Although there is considerable heterogeneity, both plots reveal high densities of lineations  
330 towards the terminus of the ice stream flow-set, where numerous smaller bedforms occur (cf.  
331 Fig. 4). However, when the cumulative length of the bedforms is included (Fig. 11b), regions  
332 of the central narrower trunk emerge as dense areas of bedforms.

333 Similar heterogeneity is seen in the data from just the DLIS transect, shown in Figure 12.  
334 There are clear regions where the number of lineations exceeds 5 per km<sup>2</sup> but intervening  
335 patches show much lower densities. The additional measurement of ‘packing’ (cumulative  
336 area per km<sup>2</sup> Fig. 12b) indicates that, in the DLIS transect, higher densities of bedforms are  
337 likely to be composed of those that are packed together quite closely (note some  
338 correspondence between high density areas in Fig. 12a and 12b), but not always.

339 The spacing of MSGLs is shown in Figure 13 in terms of the distance to the nearest  
340 neighbour both across flow (lateral) and along-flow (longitudinal) direction. Similar to  
341 histograms of their size and elongation (e.g. Figure 7), the distributions of the data are  
342 unimodal with a strong positive skew. This suggests that the MSGL have preferred lateral  
343 spacing (Fig. 13a) of between 50 to 250 m (mean = 233; median = 84 m: Table 1). The data  
344 for longitudinal spacing (Fig. 13b) is less ‘peaky’ but is, again, clearly unimodal, with most  
345 bedforms between 200 and 850 m apart (mean of 624 m, median of 429 m). A more random  
346 distribution might be expected to fill the bins on the x-axis more evenly, e.g. all bins <500 m.

347

348

#### 349 **5. Discussion: Implications for the formation of MSGL and subglacial bedforms**

350 *5.1. Size and shape characteristics of MSGL and comparison with drumlins*

351 Comprehensive mapping of the DLIS bed reveals that this flow-set contains some of the  
352 longest subglacial bedforms observed above present-day sea level. These bedforms are found  
353 in the narrower ‘trunk’ of the bottleneck flow pattern and reach lengths >20 km and  
354 elongation ratios that approach 150:1. Widths range from 39 to 553 m (mean 117 m) and  
355 lateral spacing range from 0 to 978 m (mean 233). These data fit broad descriptions of MSGL  
356 (e.g. Clark, 1993; Clark *et al.*, 2003; Ó Cofaigh *et al.*, 2005, Livingstone *et al.*, 2012), whose  
357 scale Clark (1993) suggested “renders them distinct from other ice-moulded landforms” (p.  
358 27). However, he acknowledged that his assertion of the spatial frequency of bedforms,  
359 reproduced in Figure 14a, was based on little quantitative data.

360 Our large dataset allows us to explore the spatial characteristics of MSGL and test the  
361 hypothesis that, in this location at least, they are a distinct bedform. In doing so, we suggest  
362 that there are several lines of evidence that falsify this hypothesis. Firstly, and most  
363 obviously, is that the MSGL-like features are found within a large flow-set that depicts a  
364 general pattern of less elongate bedforms immediately upstream and downstream of the  
365 longer bedforms (Fig. 4a). The high levels of parallel conformity (Fig. 5) and the lack of  
366 cross-cutting bedforms suggest that we are not viewing a mixed population of bedforms  
367 created by more than one ice flow event (i.e. one slow and one fast flow event). Second,  
368 within this broad pattern, there are clear cases of MSGL-like features sitting side by side with  
369 much smaller features that might be better described as drumlins (e.g. Fig. 4b & c). This is  
370 plainly illustrated on plots of bedform length from both the entire flow-set and the DLIS  
371 transect (Fig. 6), which overlap. Third, a comparison of our quantitative data (length, width  
372 and elongation ratio) with those from a large database of drumlins from Britain and Ireland  
373 (Clark *et al.*, 2009) also reveals populations that overlap, especially in terms of length, see

374 Figure 15. If the MSGL were a separate ‘species’ of bedform, one might expect histograms to  
375 reveal two separate populations (e.g. Fig. 14).

376 We therefore conclude that the features that fit the broad category of MSGLs on the DLIS  
377 bed are simply attenuated variants of more classic drumlins, with which they are clearly  
378 interspersed on a continuum. Indeed, the mean values for planar asymmetry are almost  
379 identical, with our MSGL-like features giving a mean value of 0.52 (90% between 0.45 and  
380 0.59) and Spagnolo’s *et al.*’s (2010) analysis of drumlins giving a value of 0.51 (81%  
381 between 0.45 and 0.55). Thus, the DLIS MSGL share characteristics with drumlins (Clark *et*  
382 *al.*, 2009) in showing a unimodal distribution of size and shape (size-specificity: cf. Evans,  
383 2010); have a short and steep lower limit, suggestive of a physical threshold for formation of  
384 the order of 100 m; and have a long, upper ‘tail’ that gradually reduces with no obvious limit  
385 or cut-off, i.e. there appears to be no physical reason why MSGLs cannot grow longer or  
386 wider.

387

## 388 *5.2. Insights regarding bedform attenuation and elongation*

389 Although there is persuasive evidence that the MSGLs on the DLIS bed are closely (probably  
390 genetically) related to shorter, less elongate drumlins, it is instructive to examine closely the  
391 ways in which they are subtly different and explore their possible evolution from shorter  
392 bedforms. Interestingly, the comparison to British and Irish drumlins (Clark *et al.*, 2009)  
393 shows that the MSGL on the DLIS bed completely overlap and simply extend the values of  
394 length (Fig. 15a). The same could be said for their elongation ratios (Fig. 15c), although  
395 there is less overlap at mid-range elongation ratios (around 5:1), which might suggest some  
396 form of ‘jump’ (rapid transition) from drumlins through to MSGL. Of most significance,  
397 however, is that the greatest differences are seen in terms of the width of the two populations

398 (Fig. 15b): British and Irish drumlins, although clearly shorter, are typically much wider than  
399 the bedforms in our DLIS transect.

400 An obvious implication is that the higher elongation ratios of the MSGL on the DLIS bed are  
401 related to their extreme length *and* their reduced width, rather than just their length. Put  
402 another way, if higher bedform elongation ratios (e.g. >10:1) are related to higher ice  
403 velocities (cf. Hart, 1999; Stokes and Clark, 2002; Briner, 2007); then one impact of rapid ice  
404 flow is to reduce bedform width as well as to enhance bedform length. This is further  
405 supported by the plots in Figure 8, which show that the longest bedforms tend to be narrowest  
406 (i.e. they are not just bigger in all dimensions: Fig. 8a) and that the widest bedforms tend to  
407 have lower elongation ratios (Fig. 8c). The fact that the width and length of MSGL does not  
408 vary in a more narrowly constrained fashion (i.e. high  $R^2$  for length versus width) suggests  
409 that they are not printed at a set shape (i.e. fixed elongation which then grows proportionally  
410 wider and longer), but that their elongation increases more quickly than their width, and  
411 smoothly and gradually. This is confirmed by a plot of the covariance of length, width and  
412 elongation ratio, shown in Figure 16, which shows a very similar sharply defined length-  
413 dependent elongation limit that was first identified by Clark *et al.* (2009) in relation to  
414 drumlins. For any given length, there is a predictable minimum value of elongation ratio  
415 below which no features are found. At its simplest, the key message is that bedforms are  
416 never both long and wide and, as such, their length must develop more quickly than their  
417 width. This supports the idea that they evolve from stubby to elongate and provides further  
418 evidence that their development is allometric, rather than isometric (cf. Evans, 2010). The  
419 discovery of the same length-dependent elongation limit for our MSGL also provides further  
420 support that they share similarities with drumlins (cf. Section 5.1).

421 It may be that MSGLs grow longer at the expense of the width, essentially by removing  
422 material on the side of the bedforms. Indeed, in our sample, bedforms with an elongation

423 ratio >40:1 are always <400 m wide, those >60:1 are always less than 300 m wide, and those  
424 >80:1 are always <200 m wide (Fig. 8c). This would suggest that fast ice flow is somehow  
425 not compatible with the formation of wide bedforms, possibly because they will generate  
426 excessive drag against the flow (cf. Spagnolo *et al.*, 2012). There is some hint that the  
427 attenuation of MSGLs may, therefore, be partly contributed to by erosional processes that  
428 removes material from between ridges, causing their width to narrow. Further support for this  
429 comes from observations reported in other studies, where lineations that are seen to be  
430 composed of mainly till are found with intervening swales extending to and exposing  
431 underlying bedrock (e.g. Clark and Stokes, 2001; Ross *et al.*, 2011). Whether material that is  
432 removed from between ridges is then recycled back into them or simply deposited further  
433 downstream beyond them is unknown, but analysis of their sedimentology on the DLIS bed  
434 suggests that their diamicton has undergone relatively short transport distances and  
435 incomplete mixing (see Paper 2: Ó Cofaigh *et al.*, submitted). Thus, their great length is  
436 unlikely to result only from subglacial deformation that transports sediment down-stream:  
437 erosional processes within the grooves must contribute to the excavation of the intra-ridge  
438 material.

439

### 440 5.3. *MSGL as part of a subglacial bedform continuum?*

441 There is compelling evidence that MSGLs on the DLIS bed are highly attenuated variants of  
442 drumlins and form an upper ‘tail’ of bedforms on histograms of length and elongation ratio,  
443 rather than a separate species (Fig. 14). This would support the idea that subglacial bedforms  
444 (e.g. ribbed moraines, drumlins, MSGLs) might represent a continuum of forms that are  
445 genetically related (see e.g. Aario, 1977; Rose, 1987), as illustrated in Figure 17. However,  
446 there are few (if any) quantitative demonstrations of a possible relationship between these  
447 bedforms, largely because workers have tended to focus on only one type and partly because,

448 until recently (e.g. Clark *et al.*, 2009), there were few studies with large enough sample sizes  
449 to provide a rigorous analysis.

450 As noted above, the most obvious explanation for the increase in bedform length is ice  
451 velocity (e.g. Hart, 1999; Ó Cofaigh *et al.*, 2002; Stokes and Clark, 2002; Briner, 2007; King  
452 *et al.*, 2009) and we suggest that, all other things being equal (e.g. sediment availability, till  
453 properties, etc.), this is the primary control on the continuum of forms. Indeed, we provide  
454 tentative predictions of the likely range of ice velocities that might account for the continuum  
455 of forms (Fig. 17), which is based on limited geophysical evidence of drumlins and MSGs  
456 forming beneath modern ice sheets, where velocities are known (e.g. King *et al.*, 2007;  
457 2009); and the observation that ribbed moraines commonly form close to ice divides  
458 (Hättestrand and Kleman, 1999). That velocity is a primary control on this continuum is also  
459 supported both by observations of gradual transitions of these forms within flow-sets as seen  
460 in this study (i.e. representing real but gradual changes in ice velocity) but also the fact that  
461 many transitions can occur abruptly (e.g. Dunlop and Clark, 2006). For example, abrupt  
462 spatial/lateral transitions from ribbed moraines to drumlins are likely to result from abrupt  
463 changes in ice velocity caused by a switch in the basal thermal regime (e.g. Dyke and Morris,  
464 1988; Dyke *et al.*, 1992; Hättestrand and Kleman, 1999). Indeed, the superimposition of  
465 ribbed moraines on the DLIS bed has been linked to ice stream shut-down and basal freeze-  
466 on (Stokes *et al.*, 2008).

467 One potential issue with the simplistic view that longer bedforms are related to fast ice flow  
468 (cf. Stokes and Clark, 2002) is that small bedforms (drumlins) can occur interspersed with  
469 much longer MSGs. A logical progression of the above argument might therefore interpret  
470 these features as localised zones of slower ice flow (basal stickiness) and, where they occur  
471 as a cluster, this might indeed be the case, especially if they clearly diverge around till free  
472 areas or bedrock bumps (cf. Stokes *et al.*, 2007; Phillips *et al.*, 2010). However, it is clear

473 from our analysis that small bedforms can occur in isolation, often sandwiched between two  
474 extremely elongate features (see Fig. 2c and 4b, 4c), which is perhaps more difficult to  
475 explain.

476 Several studies have shown that variations in bedform size and shape can arise from  
477 variations in underlying geology (Rattas and Piotrowski, 2003; Greenwood and Clark, 2010;  
478 Phillips et al., 2010). Rattas and Piotrowski (2003), for example, found that smaller and more  
479 elongate drumlins were underlain by low permeability bedrock under a small ice stream from  
480 the late Weichselian Ice Sheet, whereas larger forms corresponded to higher permeability  
481 bedrock. Major bedrock structures and changes in lithology have also been invoked to  
482 explain transitions in bedform shape and elongation ratio under parts of the Irish Sea Ice  
483 Stream (e.g. Phillips *et al.*, 2010) and, more generally, Greenwood and Clark (2010) noted  
484 coincident changes in substrate and bedform morphometry in parts of Ireland.

485 Under the DLIS, the major geological change is the transition from predominantly crystalline  
486 bedrock in the ice stream onset zone (typically massive gneissoid gneisses) to a major  
487 sedimentary basin known as the 'Thelon Formation', which underlies most of the narrower  
488 main trunk and is characterised by more easily erodible sandstones (Aylsworth and Shilts,  
489 1989b). Previous work (Stokes and Clark, 2002; 2003b, c) noted the broad correspondence  
490 between the most elongate bedforms and the Thelon sandstones, but also pointed out that the  
491 sandstones extend outside of the lateral margins of the ice stream, where no MSGS are found.  
492 Furthermore, there is no abrupt transition in bedform elongation ratios (Fig 4) that coincides  
493 with the underlying geological boundaries. We also note that whilst bedrock is close to the  
494 surface, and occasionally exposed, on parts of the ice stream bed (see Fig. 10 in paper 2: Ó  
495 Cofaigh *et al.*, submitted), there is little correspondence between the spatial variability in the  
496 underlying geology, which is of the order of 10s of kilometres (Donaldson, 1969), and the  
497 size and shape of clusters of bedforms over similarly scaled patches. Rather, our observations

498 confirm a gradual transition in length and elongation ratio along the flow-set (Fig. 4a), that is  
499 only interrupted by highly localised, often isolated, occurrences of short bedforms (e.g. 1 km  
500 long), juxtaposed next to those which can exceed 10 km in length (Fig. 4b and c).

501 Although we cannot rule out the possibility that some small bedforms were simply starved of  
502 sediment that prevented their elongation, we view it unlikely that they are a manifestation of  
503 a highly localised sticky spot and/or spatial variation in geology/sediment thickness, and  
504 instead appeal to the notion of a dynamic subglacial system (cf. Smith *et al.*, 2007; King *et*  
505 *al.*, 2009; Hillier *et al.*, 2013) whereby lineations are continually being created, remoulded  
506 and, in some cases, potentially erased. Even a relatively short-lived episode of ice flow (in  
507 this case just a few hundred years: see section 2), would create a population of bedforms of  
508 different ages; just like a snapshot of a human population. Implicit in this argument is that  
509 bedforms are created and form relatively rapidly (i.e. in decades rather than over centuries:  
510 cf. Smith *et al.*, 2007) and, under ice stream velocities (e.g.  $500 \text{ m a}^{-1}$ ), it is not inconceivable  
511 that a 50 km long MSGL could form in just 100 years. A further implication is that short  
512 bedforms can also be preserved on palaeo-ice stream beds, but only if they were ‘born’ just  
513 before ice stream shut-down (or deglaciation) and did not have time to ‘mature’.

514 In summary, if MSGL from the Dubawnt Lake ice stream are representative of the wider  
515 population of MSGL, which is yet to be demonstrated, they appear to indicate that they are  
516 genetically related to drumlins. This supports the notion of a subglacial bedform continuum  
517 (cf. Rose, 1987; Aario, 1977) that is predominantly controlled by ice velocity, but which in  
518 any given setting is likely to be confounded by the duration of flow and an evolving  
519 population of different aged bedforms. The alternative is that some of the larger variants of  
520 MSGL may plot as a separate species (i.e. significantly larger, longer, wider), but there is  
521 insufficient data to test this at present. Indeed, it is likely that the ‘needle-like’ DLIS features  
522 are at the lower end of MSGL dimensions (see for example bedform lengths and amplitudes

523 in Canals *et al.*, 2000), although this can only be verified by a more comprehensive  
524 comparison of MSGL characteristics from a variety of settings.

525

#### 526 *5.4. Qualitative comparison to existing theories of MSGL formation*

527 Various hypotheses have been put forward to explain the formation of MSGLs and these can  
528 be summarised as:

- 529 1. Subglacial deformation of till and attenuation downstream (Clark, 1993)
- 530 2. Catastrophic meltwater floods (Shaw *et al.*, 2000, 2008)
- 531 3. ‘Groove-ploughing’ by roughness elements (keels) in the basal ice (Clark *et al.*,  
532 2003)
- 533 4. Spiral flows in basal ice (Schoof and Clarke, 2008)
- 534 5. A rilling instability in the basal hydraulic system (Fowler, 2010)

535 The first two hypotheses are, essentially, extensions of ideas that have been proposed to  
536 explain drumlins and, as such, they appeal to the notion of a subglacial bedform continuum  
537 (e.g. Aario, 1977; Rose, 1987). In contrast, the other three hypotheses have departed  
538 somewhat from ideas linked to drumlin formation and have instead appealed to processes that  
539 might act to carve a grooved till surface. In this section, we review these hypotheses and  
540 discuss the extent to which they are compatible with our morphometric data (including any  
541 predictions they make).

542

##### 543 *5.4.1. Deformation of till and attenuation downstream*

544 Having formally recognised and named MSGLs, Clark (1993) discussed their possible mode  
545 of origin and suggested that it was unlikely that they formed in an almost instantaneous  
546 manner (e.g. through fluvial activity or large basal crevasses) due to their great length,

547 straight form and repetitive parallel arrangement. Rather than appeal to a new formative  
548 mechanism, Clark suggested that the extensive literature on other ice moulded bedforms  
549 provides a useful starting point and that the incremental action of ice flow in streamlining  
550 MSGL through subglacial deformation/erosion seemed to be a likely explanation. He argued  
551 that if the development of other ice-moulded bedforms, such as drumlins, could initiate by  
552 subglacial deformation around inhomogeneities in till (e.g. Boulton, 1987), then similar  
553 processes might form MSGL, with the difference in scale resulting from variations in the  
554 controlling parameters. Specifically, Clark (1993) suggested that basal ice velocities and the  
555 duration of flow are the primary controls of MSGL formation and attenuation. He then  
556 argued that it was unlikely that ice sheet flow-lines remained stable for long enough to  
557 produce MSGL and invoked a relatively rapid formation under extremely high velocities (e.g.  
558 surges or ice streams), which has since gained widespread acceptance (cf. Stokes and Clark,  
559 1999; King *et al.*, 2009). Thus, Clark (1993) took the view that MSGLs might be formed  
560 under rapid ice velocities, where high strain rates, coupled with a plentiful supply of  
561 sediment, might lead to subglacial deformation and attenuation of drumlins into much more  
562 elongate MSGLs.

563 In support of this hypothesis, the Dubawnt Lake MSGLs are formed side-by-side with  
564 drumlins and have a slight preference for classical asymmetry (Fig. 9), which suggests that  
565 they share a common origin. Furthermore, even the longest lineation on the ice stream bed  
566 (~20 km) could have formed in as little as 40 years under basal ice velocities of 500 m a<sup>-1</sup>.  
567 However, it would appear that MSGLs on the DLIS bed have a preferred spacing, and this is  
568 more difficult to reconcile with initiation from pre-existing obstacles/inhomogeneities, which  
569 are more likely to be randomly dispersed. On the other hand, perhaps a pattern of 'emergent'  
570 MSGL could arise from an instability in the deforming bed (Clark, 2010), as has been  
571 hypothesised for drumlins (Hindmarsh, 1998; Fowler, 2000, 2009; Stokes *et al.*, 2013). A

572 more rigorous test of the subglacial deformation hypothesis also requires closer inspection of  
573 the composition and internal structure of the MSGSLs, and there is evidence from sediment  
574 exposures that MSGSL on the DLIS bed are characterised by ‘cores’ that consist of crudely  
575 stratified glaciofluvial sediments, overlain by till (see Paper 2: Ó Cofaigh *et al.*, submitted).  
576 This observation suggests that any subglacial deforming bed must have eroded down into  
577 pre-existing sediments (Boyce and Eyles, 1991; Stokes *et al.*, 2013), unless these sediments  
578 were laid down during MSGSL formation.

579

#### 580 *5.4.2. Catastrophic meltwater floods*

581 Shaw *et al.* (2008) present a radically different interpretation of MSGSLs based on  
582 observations from Antarctic cross-shelf troughs and invoke catastrophic discharge of  
583 turbulent subglacial meltwater. This hypothesis has been applied to drumlin formation (e.g.  
584 Shaw, 1983) and large-scale terrestrial flutings (which could equally be termed MSGSLs:  
585 Shaw *et al.*, 2000) and Shaw *et al.* (2008). The basis for this theory is the analogy between  
586 MSGSLs and similar forms and patterns formed by broad, turbulent flows in water and air (e.g.  
587 elongate yardangs in aeolian environments, ‘rat-tails’ in fluvial environments, and  
588 megafurrows in ocean-floor sediments: see Shaw *et al.* 2008 and references therein). These  
589 flows are known to generate longitudinal vortices when they encounter an obstacle, which  
590 then acts to focus meltwater erosion around the stoss end of the resultant bedform and along  
591 their flanks. The form analogy is certainly persuasive and Shaw *et al.* (2008) strengthen their  
592 argument by pointing to the abundance of meltwater features and tunnel channels in ice  
593 stream onset zones (e.g. crescentic and hairpin scours around the stoss end of drumlins and  
594 MSGSL), and numerous gullies and channels that often characterise the continental slope.

595 We note an absence of major drainage/meltwater channels either upstream or downstream of  
596 the MSGLS on the DLIS bed. Abundant eskers are present and draped on top of the MSGL,  
597 but these are slightly misaligned with the predominant lineation direction (e.g. see Fig. 6 in  
598 Stokes and Clark, 2003b), which implies a (unknown) time interval between lineation  
599 formation and esker formation. Furthermore, the DLIS MSGL are superimposed by ribbed  
600 moraine in some places and it is difficult to envisage how one or more meltwater floods  
601 might have produced MSGL, then ribbed moraine (but without substantial modification of  
602 the underlying MSGL) and then a sequence of misaligned eskers.

603 Intriguingly, we note that some of the MSGL on the DLIS bed appear to have over-  
604 deepenings at their stoss end (e.g. Fig. 5c). However, such over-deepenings could equally  
605 form by localised subglacial meltwater erosion (hence explaining their sporadic appearance)  
606 and/or by proglacial meltwater erosion (cf. Ó Cofaigh *et al.*, 2010). There is also an issue as  
607 to whether the magnitude of meltwater required to form such floods is plausible (e.g. Clarke  
608 *et al.*, 2005). It is difficult to envisage how a flow-set ranging from 350 to 140 km in width  
609 and >450 km long could be formed by a catastrophic flood that left minimal evidence of  
610 meltwater erosional features (major channels, lag deposits, etc.). Finally, the absence of any  
611 evidence for a meltwater flood during MSGL formation under Rutford Ice Stream in West  
612 Antarctica (King *et al.*, 2009) would appear to favour a mechanism invoking ice flow  
613 interacting with soft, saturated till. Shaw and Young (2010) acknowledge that the data from  
614 King *et al.* (2009) “oblige us to take a long, hard look at the megaflood hypothesis” (p. 199)  
615 and we therefore consider it unlikely that the DLIS MSGL were formed through this  
616 mechanism (cf. Paper 2: Ó Cofaigh *et al.*, submitted).

617

618 5.4.3. ‘Groove-ploughing’

619 Based on observations that the appearance of MSGs resembles a corrugated or grooved till  
620 surface (e.g. Dean, 1953; Lemke, 1958; Heidenreich, 1964; Stokes and Clark, 2003a), Clark  
621 *et al.* (2003) proposed a ‘groove-ploughing’ hypothesis. The central tenet of this hypothesis is  
622 that the base of the ice is a rough surface (with bumps of the order  $10\text{--}10^3$ ). Indeed,  
623 observations of ‘flowstripes’ on the surface of ice streams support this view because rapidly  
624 sliding ice is exceedingly ‘transparent’ to the bed topography, i.e. if the bed is corrugated, the  
625 surface will reflect this at certain wavelengths (Gudmundsson *et al.*, 1998). Recent work has  
626 also shown that flow convergence can generate flow-stripes through transverse compressional  
627 strain and longitudinal extension, which characterises ice stream onset zones (Glasser and  
628 Gudmundsson, 2012). With this in mind, Clark *et al.* (2003) argued that major roughness  
629 elements in the ice base (referred to as ‘keels’) passing over a weak and poorly consolidated  
630 bed of soft saturated sediments (again, characteristic of most ice stream beds) could plough  
631 through these sediments and carve elongate grooves, deforming material up into intervening  
632 ridges. As Clark *et al.* (2003) note, a critical aspect of this theory is the ability of the grooves  
633 to plough through sediment for a sufficient distance (several kms) without thermodynamic  
634 and mechanical degradation. They demonstrate that that larger keels (e.g. 30 m wavelength, 5  
635 m amplitude) are more likely to survive (e.g. Thorsteinsson and Raymond, 2000) and that  
636 survival distances of 10-100 km are plausible, depending on ice velocity (Thorsteinsson and  
637 Raymond, 2000; Tulaczyk *et al.*, 2001; Clark *et al.*, 2003).

638 In order to facilitate testing of their hypothesis, Clark *et al.* (2003) make several predictions  
639 of the nature of the geomorphology of the MSG that should arise from groove-ploughing.  
640 One prediction is that MSGs should be common downstream of regions where basal ice  
641 roughness is produced (i.e. contact with hard bedrock and/or flow convergence). This  
642 prediction is certainly fulfilled for the DLIS bed, where MSGs are only located in the  
643 narrow main trunk, immediately downstream of a major zone of flow convergence (Fig. 4).

644 Although there is no obvious transition from hard bedrock to soft sediments in the ice stream  
645 onset zone (De Angelis and Kleman, 2008), we note that the DLIS bed is characterised by a  
646 relatively thin till cover (ranging from exposed bedrock to several metres thick). A further  
647 prediction is that the transverse roughness of ice stream beds should greatly exceed  
648 longitudinal roughness (Clark *et al.*, 2003) and while we have not explicitly measured or  
649 quantified roughness, it is clear that this is likely to be the case (see Fig. 5).

650 Clark *et al.* (2003) also predict that the transverse groove-spacing should be related to the  
651 spatial frequency of bedrock roughness but we are unable to test this prediction without a  
652 more thorough analysis of where bedrock roughness exists. However, very few MSGL are  
653 associated with exposed bedrock at the stoss end (e.g. Fig. 5). Elsewhere, it is also known  
654 that MSGLs occur in areas lacking bedrock outcrops and where Quaternary sediments exceed  
655 100 m in thickness, e.g. Canadian Prairies (Ross *et al.*, 2009). Thus, although we cannot rule  
656 out the possibility that bedrock obstacles may exist beneath the till surface on the DLIS, we  
657 deem this unlikely because a preferred lateral spacing (Fig. 13a) is difficult to reconcile with  
658 a preferred spacing of bedrock obstacles. Indeed, Clark *et al.* (2003) proposed that the  
659 spacing of grooves should change in proportion to the amount of roughness, with spacing  
660 between lineations greatest in the wider convergence zone, rather than the narrower main  
661 trunk. Our analysis of bedform density across the ice stream (e.g. Fig. 11) reveals no obvious  
662 pattern towards a higher density of bedforms (and intervening grooves) in the central trunk.  
663 There are low density patches in the onset zone and high densities in the narrow trunk, but  
664 there are even higher densities towards the terminus (Fig. 11a).

665 Arguably, the most critical prediction of the theory is that groove width and depth should  
666 decrease as it passes downstream, i.e. as the keel melts out, the groove becomes shallower  
667 and, as a result, the lateral edges of the two neighbouring bedforms should increase in  
668 distance downstream as they become more tapered. Although we have not measured this

669 directly, there is little evidence in the detailed mapping (e.g. Figs. 2 and 4) that neighbouring  
670 bedforms become more tapered downstream. Moreover, analysis of their plan-form (Fig. 9)  
671 suggests that most bedforms are approximately symmetric and lack a tapered lee end,  
672 although we note small clusters of bedforms that exhibit the classic asymmetry predicted by  
673 the groove-ploughing hypothesis (Fig. 10b). We also observe the initiation of bedforms  
674 within grooves (e.g. Fig. 2c), which is difficult to reconcile with groove-ploughing, unless  
675 these bedforms are seeded by roughness elements within/beneath the till layer.

676 Thus, there is some observational support for groove-ploughing, but it is also clear that this  
677 process cannot explain all of the observations and that it is likely that a more pervasive  
678 mechanism should be invoked. This same conclusion is implicit in Clark *et al.* (2003) who  
679 drew attention to an antecedent drumlinised surface which was later subjected to localised  
680 groove-ploughing (see their Fig. 3) and who also pointed out that an episode of groove-  
681 ploughing may provide the necessary relief amplification to begin to ‘seed’ subglacial  
682 bedforms. Clark *et al.* (2003) do not suppose that groove-ploughing always occurs under ice  
683 streams, but that it may occur under appropriate conditions. Such conditions may have  
684 occurred transiently on the DLIS bed and the preservation of pre-existing glaciofluvial  
685 sediments within the ridges (Paper 2: Ó Cofaigh *et al.*, submitted) is consistent with erosional  
686 processes contributing to their development.

687

#### 688 *5.4.4. Spiral flows in basal ice*

689 Schoof and Clarke (2008) proposed that subglacial flutes may be formed through a transverse  
690 secondary flow in basal ice and explore the possibility that such a mechanism could account  
691 for much larger megafutes/MSGLs. They propose that a corkscrew-like spiral flow could  
692 remove sediment from troughs between flutes and deposit it at their crest. This was first

693 suggested by Shaw and Freshauf (1973) on the basis of herringbone-type patterns in clast  
694 fabrics from within flutes (see also Rose, 1989) that were suggestive of stress patterns that  
695 indicate transport of material from interflute troughs towards flute ridges. Thus, the  
696 hypothesis shares similarities with both groove-ploughing (Clark *et al.*, 2003) and mega-  
697 floods (Shaw *et al.*, 2008) in terms of the focus on excavating grooves to build the ridges.  
698 The key departure from these hypotheses, however, is that Schoof and Clarke's (2008)  
699 treatment does not require any initiating protuberance, either in the bed or the ice, although  
700 that is not to say that such obstacles will not form bedforms when they occur.

701 Schoof and Clarke (2008) acknowledge that the generation of secondary flows in ice is not  
702 straightforward (unlike for example, in the turbulent flow of water) and so they explore ways  
703 of generating secondary flows based on a non-Newtonian rheology (i.e. departing from more  
704 standard assumptions: Paterson, 1994, chapter 5). Specifically, they require that the rheology  
705 of ice allows for the generation of deviatoric normal stresses transverse to the main ice flow  
706 direction, a characteristic of nonlinearly viscous and viscoelastic fluids described by a  
707 Reiner-Rivlin rheology. They note that the possibility of the normal stress effects they  
708 describe was acknowledged in the original paper by Glen (1958) and they also highlight  
709 experimental evidence (e.g. McTigue *et al.*, 1985) that indicates that the deviatoric stress  
710 generated by a given strain rate is not, in general, parallel to the strain rate tensor; and that  
711 simple shearing flow will generate normal stresses perpendicular to the flow direction.

712 Whilst explicitly emphasising that their hypothesis is conceptual, Schoof and Clarke (2008)  
713 demonstrate numerically that small undulations in the bed in conjunction with normal stress  
714 effects in the ice can cause the formation of such secondary flows and the subsequent  
715 amplification of the bed undulations, i.e. that the flow of ice close to the bed can be directed  
716 towards flute crests. They then explore various parameter values and speculate that small  
717 bedforms (e.g. low relief flutes) could form relatively quickly (few decades, rather than

718 centuries), which is compatible with observations (e.g. Rose, 1989). However, formation of a  
719 300 m wide MSGL would require about 1000 years, which is inconsistent with rapid  
720 evolution of bedforms reported under Rutford Ice Stream (Smith *et al.*, 2007; King *et al.*,  
721 2009) and, indeed, the longevity of the Dubawnt Lake Ice Stream (Stokes and Clark, 2003b).  
722 They concede, therefore, that the growth rates predicted by the theory, at least in its current  
723 form, are insufficient to generate the large-scale flutings formed by the major mid-latitude ice  
724 sheets; but they further point out that this conclusion is dependent on the parameterisation of  
725 subglacial sediment transport, which is only poorly understood. Thus, although it holds  
726 promise in terms of predicting assemblages of evenly spaced lineations, which our data  
727 support, we view it unlikely that the DLIS MSGL were formed through this mechanism,  
728 given their large size and the non-standard assumptions regarding ice rheology.

729

#### 730 *5.4.5. Rilling instability*

731 A rilling instability theory was recently put forward by Fowler (2010), which is an extension  
732 of the instability theory for drumlin formation (Hindmarsh, 1998; Fowler, 2000; 2009;  
733 Schoof, 2007), but which includes a dynamic description of the local subglacial drainage  
734 system. Specifically, Fowler (2010) demonstrates that a uniform water-film flowing between  
735 ice and deformable subglacial till is unstable and rilling will occur, similar to that in a  
736 subaerial setting and which results in a number of streams separated by intervening ridges. In  
737 common with mathematical treatments seeking to explain the formation of drumlins (Fowler,  
738 2000; 2009) and ribbed moraines (Dunlop *et al.*, 2008) from an unstable till layer, the theory  
739 is capable of making quantitative predictions of bedform dimensions. For the particular  
740 choice of parameters used in Fowler (2010), the preferred spacing (distance to nearest lateral  
741 neighbour) is 394 m; the preferred length scale is 52.9 km and the elevation scale is 12.3 m.

742 The predicted lateral spacing of MSGL is relatively close to that which is observed (mean of  
743 233 m: see section 4.4), but this is strongly dependent on the choice of parameters selected.  
744 The predicted length scales are also the same order of magnitude, although a predicted value  
745 of 52.9 km is much longer than is observed on the DLIS bed (max. length observed = 20.1  
746 km). As noted above, we have no systematic measurements of MSGL elevation but  
747 observations in the field show ridges typically between 5 and 15 m high, which is similar to  
748 those predicted in Fowler (2010). Furthermore, it is implicit in the rilling instability that  
749 ridges should show a preferred spacing in the transverse direction, i.e. a pattern of roughly  
750 equally spaced ridges, rather than a more random distribution. Although we have not  
751 performed a systematic analysis of bedform patterning (e.g. regular v. random) we note that  
752 the lateral spacing reveals a unimodal distribution (Fig. 13). Thus, preliminary predictions of  
753 the rilling instability appear to be consistent with the characteristics of MSGL on the DLIS  
754 bed and, as such, it appears to be a promising explanation that deserves further attempts at  
755 falsification.

756

#### 757 5.4.6. Summary

758 Four of the five existing hypotheses for MSGL formation focus primarily on the production  
759 of intervening grooves, rather than building of ridges (e.g. through ploughing of ice keels,  
760 subglacial meltwater flow, or spiral flows in basal ice), and this is consistent with our data  
761 which seems to require width to reduce as bedforms attenuate. However, no single theory is  
762 developed to the stage where it is sufficient to explain their formation. Subglacial  
763 deformation of till and attenuation downstream is plausible, but observations of stratified  
764 cores (see Paper 2: Ó Cofaigh *et al.*, submitted) suggests that this process was not pervasive,  
765 and the preferred spacing of MSGLs is unlikely to match the location of pre-existing  
766 obstacles and/or inhomogeneities. The meltwater flood theory (Shaw *et al.*, 2008) is rejected

767 on the basis of the lack of evidence of meltwater erosion (tunnel valleys, channels, lag  
768 deposits, etc.); concerns over the magnitude of water required to be stored and released; and  
769 the preservation (rather than removal by catastrophic floods), in places, of three generations  
770 of bedforming events (first MSGL, then ribbed moraines, then eskers). Notwithstanding the  
771 assumptions regarding the non-standard rheology of ice, spiral flows in basal ice (Schoof and  
772 Clarke, 2008) are also rejected because the theory, at least in its present form, is unable to  
773 grow sufficiently large MSGL within the timeframes of their generation. There is limited  
774 evidence to support groove-ploughing (Clark *et al.*, 2003), but if this process did occur, it was  
775 at most, limited in both space and time. The rilling instability theory (Fowler, 2010) shows  
776 promise in terms of predicting both the spacing and length of MSGL, but these predictions  
777 are heavily dependent on the choice of parameters and a more comprehensive evaluation of  
778 their sensitivity is yet to be undertaken.

779 Given that our data would appear to favour a subglacial bedform continuum, with MSGLs  
780 being more extreme/elongate variants of drumlins, future work might want to focus on a  
781 unifying theory that explains a range of subglacial bedforms (Stokes *et al.*, 2011), rather than  
782 appealing to 'special' circumstances to only explain MSGLs (cf. Clark, 2010). However, it  
783 should be emphasised that the data from this paper represent a single case study and, as  
784 discussed above, it may be that the MSGLs on the DLIS might be better described as  
785 drumlins. This assumes that there are two separate 'species' of bedform, which has yet to be  
786 demonstrated and this is a key area for future work to address.

787

788

## 789 **6. Conclusions**

790 This paper provides the first substantive dataset (17,038 lineations) on the size, shape and  
791 spacing of a zone of MSGLs from the central trunk of Dubawnt Lake palaeo-ice stream bed

792 (Stokes and Clark, 2003b, c). Mapping from a central transect across the width of the ice  
793 stream which incorporates, but does not arbitrarily select, the most elongate lineations  
794 indicates a mean length of 945 m (min = 186; max = 20146); a mean width of 117 m (min =  
795 39; max = 553), and a mean elongation ratio (length: width) of 8.7 (min = 2.2, max = 149.1).  
796 Analysis of their plan-form shows that most lineations are approximately symmetric, but with  
797 a very slight tendency to possess an upstream half that is larger than their downstream half.  
798 Lineations show a dominant lateral spacing, with a mean of 234 m (min = 0, max = 5104)  
799 and a slightly less dominant longitudinal spacing with a mean 625 m (min = 0.05, max =  
800 8285). The unimodal distribution of these data hints at a regular patterning of MSGLs, rather  
801 than a more random distribution, although confirmation of this awaits more rigorous analysis  
802 from other ice stream beds.

803 A key conclusion is that these data clearly show a mixed population of lineations with  
804 features characteristics of MSGL interspersed with much smaller lineations that might be  
805 more appropriately termed drumlins. Given that there is no obvious and abrupt spatial  
806 transition, we suggest that they form part of a subglacial bedform continuum (cf. Aario, 1977;  
807 Rose, 1987) and that MSGL in this location are simply an extension of drumlins. Comparison  
808 to a large database of British and Irish drumlins (Clark *et al.*, 2009) confirms this supposition,  
809 showing that our data simply extend the length and elongation range of drumlins, i.e. they do  
810 not plot as separate populations. The largest difference is found in terms of their width, with  
811 MSGLs typically much narrower than drumlins. This suggests that one impact of rapid ice  
812 flow is to create narrower bedforms as well as attenuating their length. Thus, our data  
813 strongly favour a subglacial bedform continuum that is primarily controlled by ice velocity,  
814 but which is confounded by the duration of ice flow and the fact that new bedforms are  
815 continually being created, remoulded, and, ultimately, erased. Given that the Dubawnt Lake  
816 Ice Stream only operated for a relatively short period of time (just a few hundred years:

817 Stokes and Clark, 2003c), a further implication is that MSGL formation (and subglacial  
818 bedforms more generally) are likely to be created over time-scales of decades, rather than  
819 centuries. Hence, theories of bedform creation ought to meet this requirement.

820 Comparison of our data with existing theories of MSGL formation suggest that none are  
821 wholly sufficient to explain their characteristics. We find little support for ideas based on  
822 spiral flows in basal ice (Schoof and Clarke, 2008) or catastrophic meltwater floods (Shaw et  
823 al., 2008); although neither of their proponents claim to offer a universal explanation and the  
824 former specifically acknowledge their inability to capture the rapid growth of large MSGL. It  
825 is possible that transient groove-ploughing (Clark *et al.*, 2003) occurred and we are unable to  
826 falsify a recent model presented by Fowler (2010), albeit in its infancy, that invokes a rilling  
827 instability whereby subglacial meltwater removes sediment from between neighbouring  
828 ridges. Thus, a tentative conclusion would be that the mechanism of MSGL formation occurs  
829 over decadal time-scales and involves both subglacial deformation of sediment and erosion of  
830 the intervening grooves (see also Paper 2: Ó Cofaigh *et al.*, submitted), but there is a clear  
831 requirement for further theoretical work on MSGL formation and the generation of testable  
832 predictions.

833

834

### 835 **Acknowledgements:**

836 This work was funded primarily by UK Natural Environment Research Council grants to  
837 CRS (NER/M/S/2003/00050) and MS (NE/J004766/1). Additional support was provided by a  
838 Natural Science and Engineering Research Council (NSERC) of Canada Discovery Grant to  
839 OBL. The Nunavut Research Institute is thanked for providing a scientific research license  
840 and Rob Currie, Mark Loewen and Boris Kotelewetz are thanked for their unstinting field  
841 assistance and logistical support. CRS would like to acknowledge further financial support

842 from a Philip Leverhulme Prize, which helped facilitate a sabbatical at the University of  
843 California, Santa Cruz. We thank the editor (Neil Glasser) and thoughtful reviews by Martin  
844 Ross, John Shaw (Geological Survey of Canada) and an anonymous referee.

845

846

847 **References:**

848 Aario, R. (1977) Classification and terminology of morainic landforms in Finland. *Boreas*, 6,  
849 87-100.

850 Aylsworth, J.M. and Shilts, W.W. (1989a) Bedforms of the Keewatin Ice Sheet, Canada.  
851 *Sedimentary Geology*, 62, 407-428.

852 Aylsworth, J.M. and Shilts, W.W. (1989b) Glacial features around the Keewatin Ice Divide:  
853 Districts of Mackenzie and Keewatin. *Geological Survey of Canada Paper* 88-24, 21  
854 pp.

855 Baranowski, S. (1977) Regularity of drumlin distribution and the origin of their formation.  
856 *Studia Geol. Polon.*, 52, 53-68.

857 Bird, J.B. (1953) The glaciation of central Keewatin, Northwest Territories, Canada.  
858 *American Journal of Science*, 251, 215-230.

859 Boots, B.N. and Burns, R.K. (1984) Analyzing the spatial distribution of drumlins: a two-  
860 phase mosaic approach. *Journal of Glaciology*, 30 (106), 302-307.

861 Boulton, G.S. (1987) A theory of drumlin formation by subglacial sediment deformation. In,  
862 Menzies, J. and Rose, J. (Eds) *Drumlin Symposium*. Rotterdam, A.A. Balkema, p. 25-  
863 80.

864 Boulton, G.S. and Clark, C.D. (1990) A highly mobile Laurentide ice sheet revealed by  
865 satellite images of glacial lineations. *Nature*, 346, 813-817.

866 Boyce, J.I. and Eyles, N. (1991) Drumlins carved by deforming till streams below the  
867 Laurentide ice sheet. *Geology*, 19, 787-790.

868 Bradwell, T., Stoker, M. and Krabbendam, M. (2008) Megagrooves and streamlined bedrock  
869 in NW Scotland: the role of ice streams in landscape evolution. *Geomorphology*, 97  
870 (1-2), 135-156.

871 Briner, J.P. (2007) Supporting evidence from the New York drumlin field that elongate  
872 subglacial bedforms indicate fast ice flow. *Boreas*, 36 (2), 143-147.

873 Canals, M., Urgeles, R. and Calafat, A.M. (2000) Deep sea-floor evidence of past ice streams  
874 off the Antarctic Peninsula. *Geology*, 28 (1), 31-34.

875 Chorley, R.J. (1959) The shape of drumlins. *Journal of Glaciology*, 3, 339-344.

876 Christoffersen, P. and Tulaczyk, S. (2003) Signature of palaeo-ice stream stagnation: till  
877 consolidation induced by basal freeze-on. *Boreas*, 32, 114-129.

878 Clark, C.D. (1993) Mega-scale glacial lineations and cross-cutting ice-flow landforms. *Earth  
879 Surface Processes and Landforms*, 18, 1-29.

880 Clark, C.D. (1997) Reconstructing the evolutionary dynamics of former ice sheets using  
881 multi-temporal evidence, remote sensing and GIS. *Quaternary Science Reviews*, 16  
882 (9), 1067-1092.

883 Clark, C.D. (2010) Emergent drumlins and their clones: from till dilatancy to flow  
884 instabilities. *Journal of Glaciology*, 51 (200), 1011-1025.

885 Clark, C.D. and Stokes, C.R. (2001) Extent and basal characteristics of the M'Clintock  
886 Channel Ice Stream. *Quaternary International*, 86, 81-101.

887 Clark, C.D., Tulaczyk, S.M., Stokes, C.R. and Canals, M. (2003) A groove-ploughing theory  
888 for the production of mega-scale glacial lineations, and implications for ice-stream  
889 mechanics. *Journal of Glaciology*, 49, 240-256.

890 Clark, C.D., Hughes, A.L.C., Greenwood, S.L., Spagnolo, M. and Ng, F.S.L. (2009) Size and  
891 shape characteristics of drumlins, derived from a large sample, and associated scaling  
892 laws. *Quaternary Science Reviews*, 28 (7-8), 677-692.

893 Clarke, G.K.C., Leverington, D.W., Teller, J.T., Dyke, A.S., Marshall, S.J. (2005) Fresh  
894 arguments against the Shaw megaflood hypothesis. A reply to comments by David  
895 Sharpe on ‘Paleohydraulics of the last outburst from glacial Lake Agassiz and the  
896 8200 BP cold event’. *Quaternary Science Reviews*, 24, 1533-1541.

897 Craig, B.G. (1964) Surficial geology of east-central District of Mackenzie. *Geological Survey  
898 of Canada Bulletin*, 99, 1-41.

899 Dean, W.G. (1953) The drumlinoid land forms of the Barren Grounds. *Canadian  
900 Geographer*, 1, 19-30.

901 De Angelis, H. and Kleman, J. (2008) Palaeo-ice stream onsets: examples from the north-  
902 eastern Laurentide Ice Sheet. *Earth Surface Processes and Landforms*, 33 (4), 560-  
903 572.

904 Donaldson, J.A. (1969) Geology, Central Thelon Plain, Districts of Keewatin and Mackenzie.  
905 Geological Survey of Canada, Preliminary Map 16-1968, 1969, 1 sheet.

906 Dyke, A.S and Morris, T.F. (1988) Canadian Landform Examples, 7. Drumlin fields,  
907 dispersal trains, and ice streams in Arctic Canada. *Canadian Geographer*, 32 (1), 86-  
908 90.

909 Dyke, A.S., Morris, T.F., Green, E.C. and England, J. (1992) *Quaternary geology of Prince  
910 of Wales Island, Arctic Canada*. Geological Survey of Canada, 433.

911 Dunlop, P. and Clark, C.D. (2006) The morphological characteristics of ribbed moraine.  
912 *Quaternary Science Reviews*, 25 (13-14), 1668-1691.

913 Dunlop, P., Clark, C.D. and Hindmarsh, R.C.A. (2008) Bed ribbing instability explanation:  
914 testing a numerical model of ribbed moraine formation arising from the coupled flow

915 of ice and subglacial sediment. *Journal of Geophysical Research*, 113 (F3), F03005,  
916 doi: 10.1029/2007JF000954).

917 Dyke, A.S., Moore, A. and Robertson, L. (2003) Deglaciation of North America. *Geological*  
918 *Survey of Canada Open File 1574*.

919 Evans, I.S. (2010) Allometry, scaling and scale-specificity of cirques, landslides and other  
920 landforms. *Transactions of the Japanese Geomorphological Union*, 31 (2), 133-153.

921 Fowler, A.C. (2000) An instability mechanism for drumlin formation. In, Maltman, A.,  
922 Hambrey, M.J., Hubbard, B. (Eds) *Deformation of Glacial Materials*. Special  
923 Publication of the Geological Society, 176. The Geological Society, London, p. 307-  
924 319.

925 Fowler, A.C. (2009) Instability modelling of drumlin formation incorporating lee-side cavity  
926 growth. *Proceedings of the Royal Society of London, Series A*, 466 (2121), 2673-  
927 2694.

928 Fowler, A.C. (2010) The formation of subglacial streams and mega-scale glacial lineations.  
929 *Proceedings of the Royal Society of London, Series A*, 466 (2123), 3181-3201.

930 Glasser, N.F. and Gudmundsson, G.H. (2012) Longitudinal surface structures (flowstripes)  
931 on Antarctic glaciers. *The Cryosphere*, 6, 383-391.

932 Glen, J.W. (1958) The flow of ice: a discussion of the assumptions made in glacier theory,  
933 their experimental foundation and consequences. In, *Physics of the Movement of Ice –*  
934 *Symposium at Chamonix, 1958, IASH Publication*, 47, 171-183.

935 Graham, A.G.C., Larter, R.D., Gohl, K., Hillenbrand, C-D., Smith, J.A. and Kuhn, G. (2009)  
936 Bedform signature of a West Antarctic palaeo-ice stream reveals a multi-temporal  
937 record of flow and substrate control. *Quaternary Science Reviews*, 28, 2774-2793.

938 Greenwood, S.L. and Clark, C.D. (2010) The sensitivity of subglacial bedform size and  
939 distribution to substrate lithological control. *Sedimentary Geology*, 232, 130-144.

940 Gudmundsson, G.H., Raymond, C.F. and Bidschadler, R. (1998) The origin and longevity of  
941 flow stripes on Antarctic ice streams. *Annals of Glaciology*, 27, 145-152.

942 Hart, J.K. (1999) Identifying fast ice flow from the landform assemblages in the geological  
943 record: a discussion. *Annals of Glaciology*, 28, 59-66.

944 Hättestrand, C. and Kleman, J. (1999) Ribbed moraine formation. *Quaternary Science*  
945 *Reviews*, 18, 43-61.

946 Heidenreich, C. (1964) Some observations on the shape of drumlins. *Canadian Geographer*,  
947 8, 101-107.

948 Hess, D.P., Briner, J.P. (2009) Geospatial analysis of controls on subglacial bedform  
949 morphometry in the New York drumlin field — implications for Laurentide Ice Sheet  
950 dynamics. *Earth Surface Processes and Landforms*, 24, 1126–1135.

951 Hillier, J.K., Smith, M.J., Clark, C.D., Stokes, C.R. and Spagnolo, M. (2013) Subglacial  
952 bedforms reveal an exponential size-frequency distribution. *Geomorphology*, 190, 82-  
953 91.

954 Hindmarsh, R.C.A. (1998) The stability of a viscous till sheet coupled with ice flow,  
955 considered at wavelengths less than the ice thickness. *Journal of Glaciology*, 44, 285-  
956 292.

957 Jezek, K., Wu, X., Gogineni, P., Rodríguez, E., Freeman, A., Rodriguez-Morales, and Clark,  
958 C.D. (2011) Radar images of the bed of the Greenland Ice Sheet. *Geophysical*  
959 *Research Letters*, 38 (1), doi: 10.1029/2010GL045519.

960 King, E.C., Woodward, J. and Smith, A.M. (2007) Seismic and radar observations of  
961 subglacial bedforms beneath the onset zone of Rutford Ice Stream, Antarctica.  
962 *Journal of Glaciology*, 53 (183), 665-672.

963 King, E.C., Hindmarsh, R.C.A. and Stokes C.R. (2009) Formation of mega-scale glacial  
964 lineations observed beneath a West Antarctic ice stream. *Nature Geoscience*, 2, 585-  
965 588.

966 Kleman, J. and Borgström, I. (1996) Reconstruction of palaeo-ice sheets: the use of  
967 geomorphological data. *Earth Surface Processes and Landforms*, 21, 893-909.

968 Lemke, R.W. (1958) Narrow linear drumlins near Velva, North Dakota. *American Journal of*  
969 *Science*, 256, 270-283.

970 Livingstone, S.J., O’Cofaigh, C.O., Stokes, C.R., Hillenbrand, C-D., Vieli, A. and Jamieson,  
971 S.R. (2012) Antarctic palaeo-ice streams. *Earth-Science Reviews*, 111, 90-128.

972 McMartin, I. and Henderson, P.J. (2004) Evidence from Keewatin (central Nunavut) for  
973 paleo-ice divide migration. *Géographie physique et Quaternaire*, 58 (2/3), 163-186.

974 McTigue, D.F., Passman, S.L. and Jones, S.J. (1985) Normal stress effects in the creep of ice.  
975 *Journal of Glaciology*, 33 (115), 268-273.

976 Ó Cofaigh, C., Pudsey, C.J., Dowdeswell, J.A. and Morris, P. (2002) Evolution of subglacial  
977 bedforms along a paleo-ice stream, Antarctic Peninsula continental shelf. *Geophysical*  
978 *Research Letters*, 29, 1199, doi 10.1029/2001GL014488.

979 Ó Cofaigh, C., Dowdeswell, J.D., Allen, C.S., Hiemstra, J.F., Pudsey, C.F., Evans, J. and  
980 Evans, D.J.A. (2005) Flow dynamics and till genesis associated with a marine-based  
981 Antarctic palaeo-ice stream. *Quaternary Science Reviews*, 24, 709-740.

982 Ó Cofaigh, C., Dowdeswell, J.D., King, E.C., Anderson, J.B., Clark, C.D., Evans, D.J.A.,  
983 Evans, J., Hindmarsh, R.C.A., Larter, R.D. & Stokes, C.R. (2010) Comment on Shaw  
984 J., Pugin, A. and Young, R. (2008): “A meltwater origin for Antarctic shelf bedforms  
985 with special attention to megalineations”, *Geomorphology* 102, 364–375.  
986 *Geomorphology*, 117, 195-198.

- 987 Ó Cofaigh, C., Stokes, C.R., Lian, O.B., Clark, C.D. and Tulaczyk, S.M. (submitted)  
988 Formation of mega-scale glacial lineations on the Dubawnt Lake Ice Stream bed: 2.  
989 Sedimentology and stratigraphy. *Quaternary Science Reviews*.
- 990 Paterson, W.S.B. (1994) *The Physics of Glaciers* (3<sup>rd</sup> Ed). Pergamon, Oxford, London.
- 991 Phillips, E., Everest, J. and Diaz-Doce, D. (2010) Bedrock controls on subglacial landform  
992 distribution and geomorphological processes: Evidence from the Late Devensian Irish  
993 Sea Ice Stream. *Sedimentary Geology*, 232, 98-118.
- 994 Prest, V.K., Grant, D.R. and Rampton, V.N. (1968) Glacial Map of Canada. Geological  
995 Survey of Canada, Map 1253A, scale 1:5,000,000.
- 996 Pritchard, H.D., Arthern, R.J., Vaughan, D.G. and Edwards, L.A. (2009) Extensive dynamic  
997 thinning on the margins of the Greenland and Antarctic ice sheets. *Nature*, 461  
998 (7266), 971-975.
- 999 Rattas, M. and Piotrowski, J.A. (2003) Influence of bedrock permeability and till grain size  
1000 on the formation of the Saadjärve drumlin field, Estonia, under an east-Baltic  
1001 Weichsealian ice stream. *Boreas*, 32, 167-177.
- 1002 Rose, J. (1987) Drumlins as part of a glacier bedform continuum. In, Menzies, J. and Rose, J.  
1003 (Eds) *Drumlin Symposium*. Rotterdam, A.A. Balkema, p. 103-116.
- 1004 Rose, J. (1989) Glacier stress patterns and sediment transfer associated with the formation  
1005 of superimposed flutes. *Sedimentary Geology*, 62, 151-176.
- 1006 Ross, M., Campbell, J.E., Parent, M. and Adams, R.S. (2009) Palaeo-ice streams and the  
1007 subglacial landscape mosaic of the North American mid-continental prairies. *Boreas*,  
1008 38, 421-339.
- 1009 Ross, M., Lajeunesse, P. and Kosar, A. (2011) The subglacial record of northern Hudson  
1010 Bay: insights into the Hudson Strait Ice Stream catchment. *Boreas*, 40 (1), 73-91.

- 1011 Schoof, C. (2007) Pressure-dependent viscosity and interfacial instability in coupled ice-  
1012 sediment flow. *Journal of Fluid Mechanics*, 570, 227-252.
- 1013 Schoof, C. And Clarke, G.K.C. (2008) A model for spiral flows in basal ice and the formation  
1014 of subglacial flutes based on a Reiner-Rivlin rheology for glacial ice. *Journal of*  
1015 *Geophysical Research*, 113, B05204.
- 1016 Shaw, J. (1983) Drumlin formation related to inverted melt-water erosional marks. *Journal of*  
1017 *Glaciology*, 29 (103), 461-479.
- 1018 Shaw, J. and Freschauf, R.C. (1973) A kinematic discussion of the formation of glacial  
1019 flutings. *Canadian Geographer*, 17 (1), 19-35.
- 1020 Shaw, J. and Young, R.R. (2010) Reply to comment by Ó Cofaigh, Dowdeswell, King,  
1021 Anderson, Clark, DJA Evans, J. Evans, Hinidmarsh, Lardner [sic] and Stokes  
1022 “Comments on Shaw, J., Pugin, A., Young, R. (2009): A meltwater origin for  
1023 Antarctic Shelf bedforms with special attention to megalineations.” *Geomorphology*,  
1024 102, 364-375. *Geomorphology*, 117, 199-201.
- 1025 Shaw, J., Faragini, D.M., Kvill, D.R., and Rains, B.R. (2000) The Athabasca fluting field,  
1026 Alberta, Canada: implications for the formation of large-scale fluting (erosional  
1027 lineations). *Quaternary Science Reviews*, 19 (10), 959-980.
- 1028 Shaw, J., Pugin, A. and Young, R.R. (2008) A meltwater origin for Antarctic shelf bedforms  
1029 with special attention to megalineations. *Geomorphology*, 102, 364-375.
- 1030 Shipp, S.S., Anderson, J.B. and Domack, E.W. (1999) Late Pleistocene-Holocene retreat of  
1031 the West Antarctic ice-sheet system in the Ross Sea: Part 1 – geophysical results.  
1032 *Geological Society of America, Bulletin*, 111 (10), 1486-1516.
- 1033 Smalley, I.J. and Unwin, D.J. (1968) The formation and shapes of drumlins and their  
1034 distribution and orientation in drumlin fields. *Journal of Glaciology*, 7, 377-390.

1035 Smith, A., Murray, T., Nicholls, K., Makinson, K. and Adalgeirsdottir, G. (2007) rapid  
1036 erosion, drumlin formation, and changing hydrology beneath an Antarctic ice stream.  
1037 *Geology*, 35 (2), 127-130.

1038 Spagnolo, M., Clark, C.D., Hughes, A.L.C., Dunlop, P. and Stokes, C.R. (2010) The planar  
1039 shape of drumlins. *Sedimentary Geology*, 232, 119-129.

1040 Spagnolo, M., Clark, C.D., Hughes, A.L.C. and Dunlop, P. (2011) The topography of  
1041 drumlins: assessing their long profile shape. *Earth Surface Processes and Landforms*,  
1042 36, 790-804.

1043 Spagnolo, M., Clark, C.D. and Hughes, A.L.C. (2012) Drumlin relief. *Geomorphology*, 153-  
1044 154, 179-191.

1045 Stokes, C.R. and Clark, C.D. (1999) Geomorphological criteria for identifying Pleistocene ice  
1046 streams. *Annals of Glaciology*, 28, 67-74.

1047 Stokes, C.R. and Clark, C.D. (2002) Are long subglacial bedforms indicative of fast ice flow?  
1048 *Boreas*, 31, 239-249.

1049 Stokes, C.R. & Clark, C.D. (2003a) Giant glacial grooves detected on Landsat ETM+ satellite  
1050 imagery. *International Journal of Remote Sensing*, 24 (5), 905-910.

1051 Stokes, C.R. and Clark, C.D. (2003b) The Dubawnt Lake palaeo-ice stream: evidence for  
1052 dynamic ice sheet behaviour on the Canadian Shield and insights regarding the  
1053 controls on ice stream location and vigour. *Boreas*, 32, 263-279.

1054 Stokes, C.R. and Clark, C.D. (2003c) Laurentide ice streaming on the Canadian Shield: A  
1055 conflict with the soft-bedded ice stream paradigm? *Geology*, 31 (4), 347-350.

1056 Stokes, C.R. and Clark, C.D. (2004) Evolution of late glacial ice-marginal lakes on the  
1057 northwestern Canadian Shield and their influence on the location of the Dubawnt  
1058 Lake palaeo-ice stream. *Palaeogeography, Palaeoclimatology, Palaeoecology*, 215,  
1059 155-171.

1060 Stokes, C.R. Clark, C.D. Lian, O. & Tulaczyk, S. (2006) Geomorphological Map of ribbed  
1061 moraine on the Dubawnt Lake Ice Stream bed: a signature of ice stream shut-down?  
1062 *Journal of Maps*, 2006, 1-9.

1063 Stokes, C.R. Clark, C.D. Lian, O. & Tulaczyk, S. (2007) Ice stream sticky spots: a review of  
1064 their identification and influence beneath contemporary and palaeo-ice streams.  
1065 *Earth-Science Reviews*, 81, 217-249.

1066 Stokes, C.R., Lian, O.B., Tulaczyk, S. & Clark, C.D. (2008) Superimposition of ribbed  
1067 moraines on a palaeo-ice stream bed: implications for ice stream dynamics and shut-  
1068 down. *Earth Surface Processes and Landforms*, 33, 4, 593-609.

1069 Stokes, C.R., Spagnolo, M. and Clark, C.D. (2011) The composition and internal structure of  
1070 drumlins: complexity, commonality, and implications for a unifying theory of their  
1071 formation. *Earth-Science Reviews*, 107, 398-422.

1072 Stokes, C.R., Fowler, A.C., Clark, C.D., Hindmarsh, R.C.A. and Spagnolo, M. (2013) The  
1073 instability theory of drumlin formation and its explanation of their varied composition  
1074 and internal structure. *Quaternary Science Reviews*, 62, 77-96.

1075 Thorsteinsson, T. and Raymond, C.F. (2000) Sliding versus till deformation in the fast  
1076 motion of an ice stream over a viscous till. *Journal of Glaciology*, 46 (155), 633-640.

1077 Tulaczyk, S.M., Scherer, R.P. and Clark, C.D. (2001) A ploughing model for the origin of  
1078 weak tills beneath ice streams: a qualitative treatment. *Quaternary International*, 86  
1079 (1), 59-70.

1080 Tyrrell, J.B. (1906) report on the Dubawnt, Ferguson, and Kazan Rivers. *Geological Survey  
1081 of Canada Annual Report*, 9.

1082 Wellner, J.S., Heroy, D.C. and Anderson, J.B. (2006) The death mask of the Antarctic ice  
1083 sheet: comparison of glacial geomorphic features across the continental shelf.  
1084 *Geomorphology*, 75, 157-171.



1086 **Tables:**

1087

1088 **Table 1: Summary statistics of lineation characteristics from the DLIS transect (see Fig.**

1089 **2 for location).**

1090

<b>Statistic</b>	<b>Length (m)</b>	<b>Width (m)</b>	<b>Elongation ratio</b>	<b>Planar asymmetry (<math>As_{pl\_a}</math>)</b>	<b>Distance to lateral nearest neighbour (m)*</b>	<b>Distance to longitudinal nearest neighbour (m)</b>
<i>n</i>	17,038	17,038	17,038	17,016 <sup>#</sup>	11,810	7,731*
<i>Minimum</i>	186	39	2.2	0.31	0	0.05
<i>5<sup>th</sup> percentile</i>	334	61	4.1	0.45	9	40
<i>25<sup>th</sup> percentile</i>	506	79	6	0.49	37	173
<i>Modal class</i>	500-600 (13%)	80-90 (15%)	5-6 (16%)	0.50-0.52 (19%)	0-50 (34%)	50-100 (8%)
<i>Mean</i>	945	117	8.7	0.52	234	625
<i>Median</i>	712	96	7.2	0.52	84	430
<i>75<sup>th</sup> percentile</i>	1,084	122	10	0.55	245	874
<i>95<sup>th</sup> percentile</i>	2,248	195	17.6	0.59	978	1,829
<i>Maximum</i>	20,146	553	149	0.73	5,104	8,285
<i>St. deviation</i>	866	45	6	0.04	411	637

1091 <sup>#</sup> The population (n) for these calculations is less than the total population (17,038) because some thin bedforms  
1092 displayed a slight curvature which meant that the mid-point used as part of the automated calculations lay  
1093 outside the polygon. As such, they were excluded.

1094 \*The population (n) for these calculations is less than the total population (17,038) because some polygons did  
1095 not have an obvious nearest neighbour and because reciprocal nearest neighbours were excluded.

1096

1097

1098

1099 **Figure Captions:**

1100

1101 **Figure 1:** Location of the Dubawnt Lake palaeo-ice stream within the region of the former  
1102 North American Laurentide Ice Sheet. Margin position and proglacial lake extent at 8.5 <sup>14</sup>C  
1103 yr BP (9.5 cal ka BP) are taken from Dyke *et al.* (2003), which is just prior to the initiation of  
1104 streaming flow. As the western margin retreated to the south-east, proglacial lakes formed  
1105 over the Canadian Shield and are thought to have triggered a short-lived episode of streaming  
1106 (few hundred years) that had ceased by 8.2 <sup>14</sup>C yr BP (cf. Stokes and Clark, 2003b; Stokes  
1107 and Clark, 2004).

1108

1109 **Figure 2:** (a) Extent of the Dubawnt Lake ice stream flow-set is shown in red (from Kleman  
1110 and Borgström, 1996; Stokes and Clark, 2003b) and coverage of Landsat satellite imagery is  
1111 shown in light grey boxes. Every lineation within the Dubawnt lake flow-set (red outline)  
1112 was mapped as a line and a central transect of these lineations was mapped as polygons (dark  
1113 grey box: DLIS transect). An example of the Landsat imagery (path 039, row 015) is shown  
1114 in (b), alongside mapped polygons in (c); location shown by yellow box in (a).

1115

1116 **Figure 3:** Illustration of the different parameters extracted from the GIS database of  
1117 lineations mapped as polygons in (a):  $A$  = area;  $L$  = length;  $W$  = width;  $U$  = upstream limit;  $I$   
1118 = intersection of  $L$  and  $W$ ;  $M$  = mid-point of  $L$ ;  $D$  = downstream limit. To measure the planar  
1119 symmetry, the shape of the bedform was divided into an upstream and downstream half and  
1120 calculated as:  $As_{pl\_a} = (A_{up}/A)$ , where  $A_{up}$  = upstream area. Higher values indicate upstream  
1121 halves that are larger than downstream halves (i.e. classically asymmetric (b)) and lower  
1122 values indicate downstream halves that are larger than upstream halves (i.e. reversed  
1123 asymmetry (d)). A perfectly symmetric case ( $As_{pl\_a} = 0.5$ ) is shown in (c).

1124

1125 **Figure 4:** (a) Glacial lineations on the DLIS bed shaded according to their length ( $n =$   
1126 42,583). Note the shorter lineations in the onset zone and, especially, towards the terminus,  
1127 with the longest lineations in the narrower main trunk. This area was selected for more  
1128 detailed mapping of the lineations as polygons (black rectangle) and an extract of this  
1129 mapped area is shown shaded according to both length (b) and elongation ratio (c).

1130

1131 **Figure 5:** Landsat imagery (path 039, row 015) of highly elongate MSGL in the central trunk  
1132 of the ice stream (a) and oblique aerial photographs of parts of the image in (b) and (c)  
1133 (photographs: C. R. Stokes).

1134

1135 **Figure 6:** Histograms of lineation length from the line database and the polygon database.  
1136 Note that both populations show unimodal distributions with a strong positive skew.  
1137 Although the polygon database clearly contains longer MSGL, this area of the ice stream bed  
1138 also contains smaller lineations. Bin size is 100 m.

1139

1140 **Figure 7:** Histograms and summary statistics of the DLIS transect for length (a), width (b),  
1141 and elongation ratio (c). Bin sizes are 100 m, 10 m and 1, respectively. Box-and-whisker  
1142 plots show the 25 and 75<sup>th</sup> percentiles (grey box), the 10<sup>th</sup> and 90<sup>th</sup> percentiles (whisker ends)  
1143 and the 5<sup>th</sup> and 95<sup>th</sup> percentiles (black dots). The mean (horizontal line) and median (dashed  
1144 horizontal line) are also shown.

1145

1146 **Figure 8:** Relationships between bedform length versus width (a), length versus elongation  
1147 ratio (b) and elongation ratio versus width (c) for the DLIS transect data ( $n = 17,038$ ). Black

1148 lines represent linear fits to the data clouds whereas red gives a power law function.  
1149 Exponential fits gave very low  $r^2$  values ( $<0.15$ ) for all plots and, for clarity, are not shown.

1150

1151 **Figure 9:** Histogram and summary statistics for a simple measurement of the planar (plan  
1152 form) asymmetry of bedforms within the DLIS transect ( $n = 17,038$ ). A value of 0.5 indicates  
1153 a perfectly symmetrical shape. Higher values indicate upstream halves that are larger than  
1154 downstream halves (i.e. classically asymmetric: Fig. 3b) and lower values indicating  
1155 downstream halves that are larger than upstream halves (i.e. reversed asymmetry: Fig. 3d).  
1156 Bin size is 0.2. Box-and-whisker plot shows the 25 and 75<sup>th</sup> percentiles (grey box), the 10<sup>th</sup>  
1157 and 90<sup>th</sup> percentiles (whisker ends) and the 5<sup>th</sup> and 95<sup>th</sup> percentiles (black dots). The mean  
1158 (horizontal line) and median (dashed horizontal line) are also shown (overlapping).

1159

1160 **Figure 10:** Glacial lineations from the DLIS transect shaded according to their planar shape.  
1161 Most lineations are approximately symmetrical in plan form (yellow: Fig. 3c), but there are  
1162 isolated cases of those that show both reverse asymmetry (blue: Fig. 3d) and classic  
1163 asymmetry (red: Fig. 3b), the latter sometimes clustering in groups of 5-10 bedforms, while  
1164 the former are much more rare and more likely to be isolated.

1165

1166 **Figure 11:** Plots of lineation density (point per unit area) in (a) and cumulative lineation  
1167 length per unit area in (b) across the entire DLIS flow-set. Although there is considerable  
1168 heterogeneity, both plots reveal high densities of lineations towards the terminus of the flow-  
1169 set, where numerous smaller bedforms occur (cf. Fig. 4). When the cumulative length of the  
1170 bedforms is included (b), regions of the central narrower trunk emerge as dense areas of  
1171 bedforms. Note that edge effects are unavoidable and the red fringe is an artefact created by  
1172 areas of zero bedforms outside the flow-set limit.

1173

1174 **Figure 12:** Plot of lineation density (point per unit area) in (a) and lineation packing (total  
1175 bedform area per unit area) in (b) for the DLIS transect. The data are highly heterogeneous,  
1176 mostly likely reflecting postglacial fluvial activity carving major river valleys and the  
1177 presence of large lakes. The additional measurement of ‘packing’ shows a broadly similar  
1178 trend to density. Note that edge effects are unavoidable and the red fringe is an artefact  
1179 created by areas of zero bedforms outside the transect limit.

1180

1181 **Figure 13:** Histograms and summary statistics of distance between bedforms in the DLIS  
1182 transect both perpendicular (a) and parallel (b) to ice flow. These data hint at a preferred  
1183 spacing of MSGLs of between 50-250 m apart from their nearest lateral neighbour and 200-  
1184 850 m for their nearest neighbour along-flow. Bin sizes are 50 m. Box-and-whisker plots  
1185 show the 25 and 75<sup>th</sup> percentiles (grey box), the 10<sup>th</sup> and 90<sup>th</sup> percentiles (whisker ends) and  
1186 the 5<sup>th</sup> and 95<sup>th</sup> percentiles (black dots). The mean (horizontal line) and median (dashed  
1187 horizontal line) are also shown.

1188

1189 **Figure 14:** Two possibilities regarding the morphometric characteristics of subglacial  
1190 bedforms: the first (a) is redrawn from Clark (1993) and views different bedforms as separate  
1191 species, with clearly preferred size and shape characteristics. The second (b) appeals to a  
1192 subglacial bedform continuum (see also Fig. 17), with the each landform genetically related,  
1193 and with size and shape characteristics falling within one population. The prevailing  
1194 paradigm is probably that shown in (a), largely because we have, perhaps unfortunately (but  
1195 understandably), given genetically similar bedforms different names, that reflect their size  
1196 and shape, which has, in turn, caused many workers to study them separately. In this paper,

1197 data appear to indicate that MSGL, at least on the DLIS bed, are simply an extension/variant  
1198 of highly attenuated drumlins, i.e. scenario shown in (b).

1199

1200 **Figure 15:** Histograms and summary statistics of the DLIS transect length (a), width (b) and  
1201 elongation ratio (c) alongside a large database of British drumlins from Clark *et al.* (2009).  
1202 DLIS MSGLs are, generally, longer and more elongate, although the populations clearly  
1203 overlap. The most important difference is that the MSGLs are narrower than drumlins, which  
1204 helps explain the weak correlation between length and width for MSGL, compared to  
1205 drumlins (cf. Fig. 8a). Box-and-whisker plots show the 25 and 75<sup>th</sup> percentiles (grey box), the  
1206 10<sup>th</sup> and 90<sup>th</sup> percentiles (whisker ends) and the 5<sup>th</sup> and 95<sup>th</sup> percentiles (black dots). The  
1207 mean (horizontal line) and median (dashed horizontal line) are also shown.

1208

1209 **Figure 16:** Plot of co-variation of length, width and elongation ratio for the DLIS transect.  
1210 Note the sharply defined length-dependent elongation ratio that was also identified by Clark  
1211 *et al.* (2009) for drumlins. This indicates that a given bedform can only extend to (attain) a  
1212 certain elongation ratio if its length also extends at a greater rate than does its width. The  
1213 identification of this same scaling law supports the idea that MSGL are genetically related to  
1214 drumlins and that they evolve allometrically (cf. Evans, 2010) from stubby to elongate.

1215

1216 **Figure 17:** Schematic representation of a subglacial bedform continuum modified from Aario  
1217 (1977); see also Rose (1987). With this view, a whole spectrum (based on shape) of  
1218 subglacial bedforms are genetically related (i.e. Fig. 14b, rather than 14a) and merge from  
1219 one into the other, e.g. from ribbed moraines through to drumlins through to MSGL. All other  
1220 things being equal (e.g. sediment availability, till properties, etc.) the most obvious control on  
1221 where a bedform lies along this continuum is ice velocity (see text for discussion).



**Figure 1:**

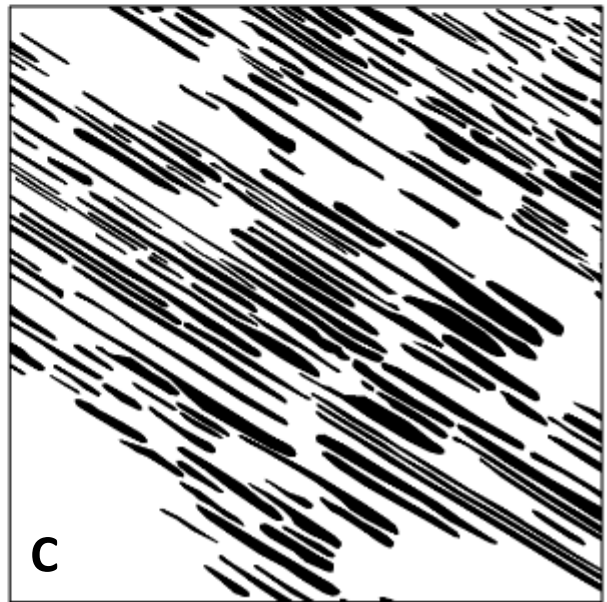
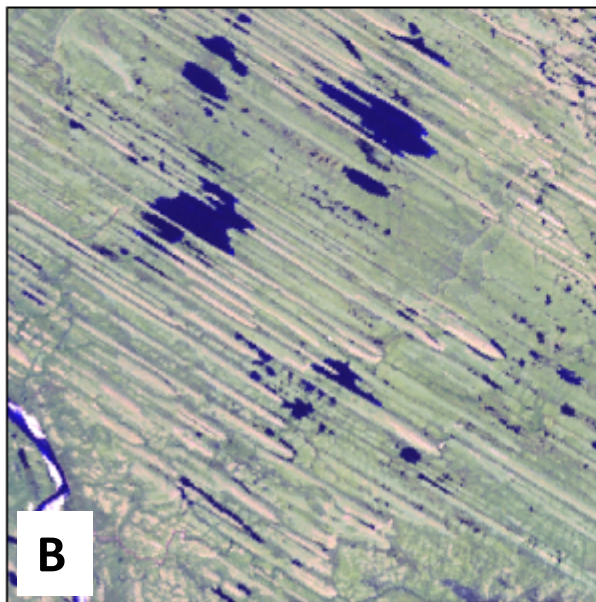
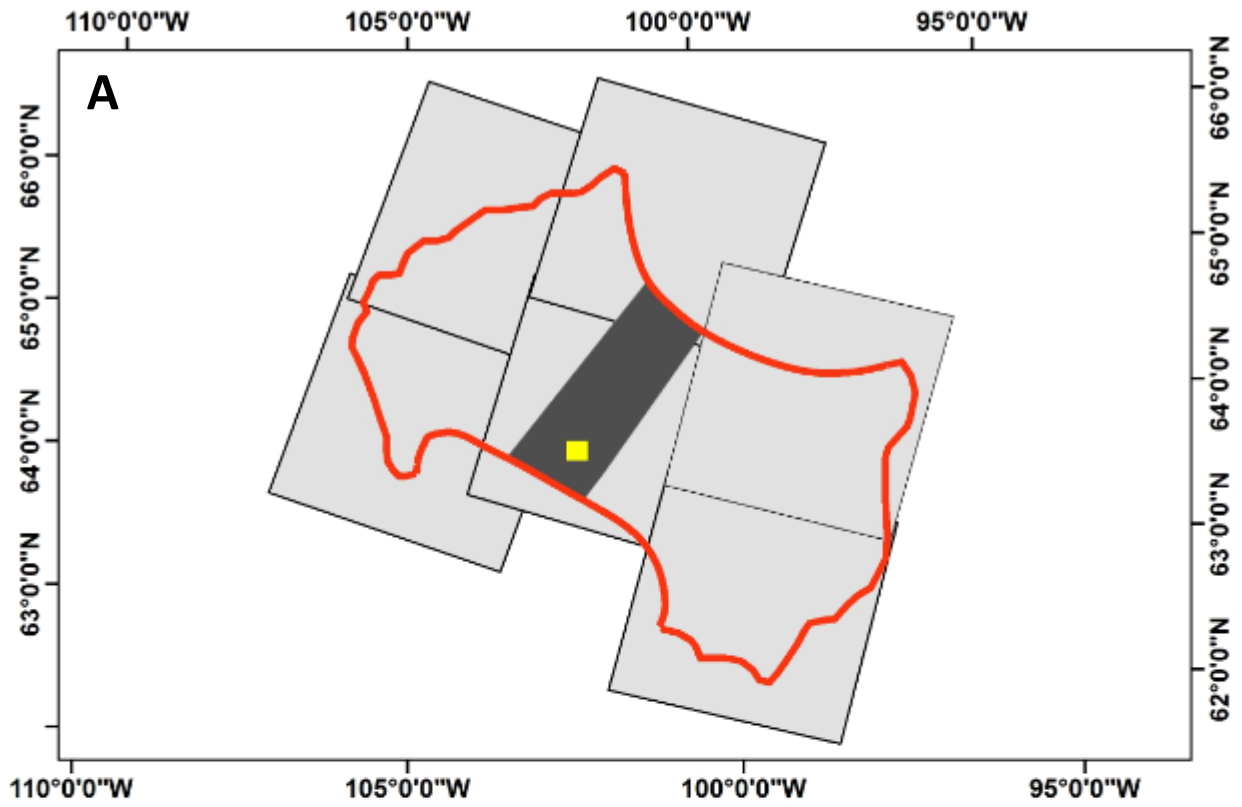


Figure 2:

← Ice flow direction

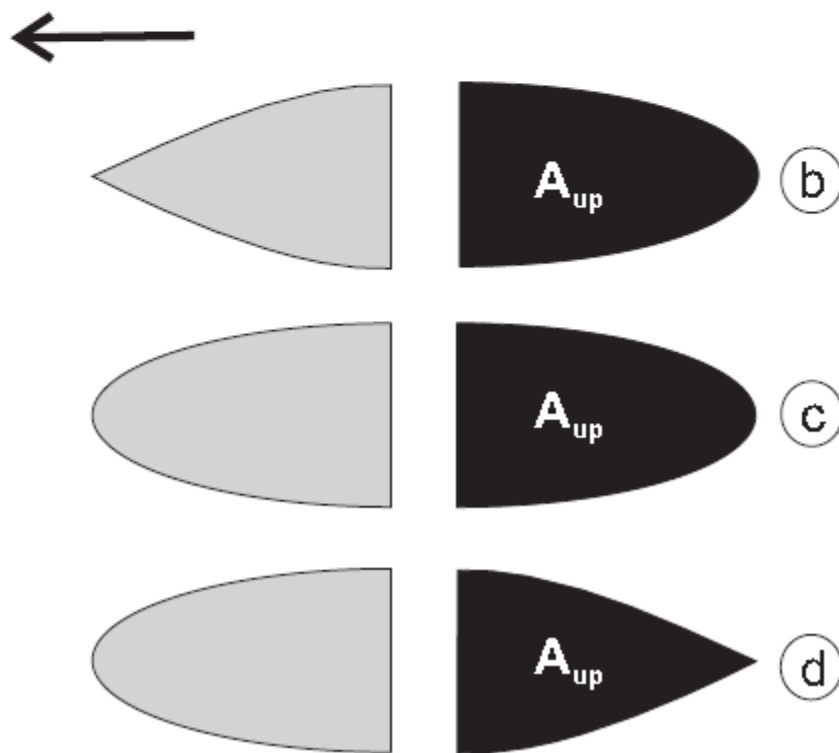
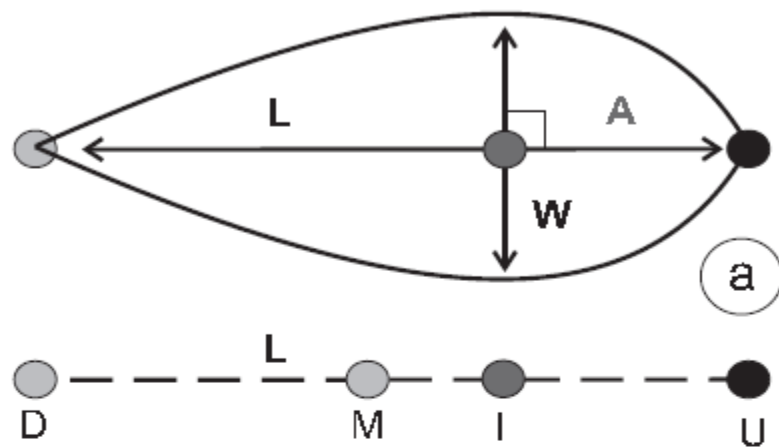


Figure 3:

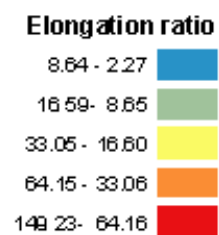
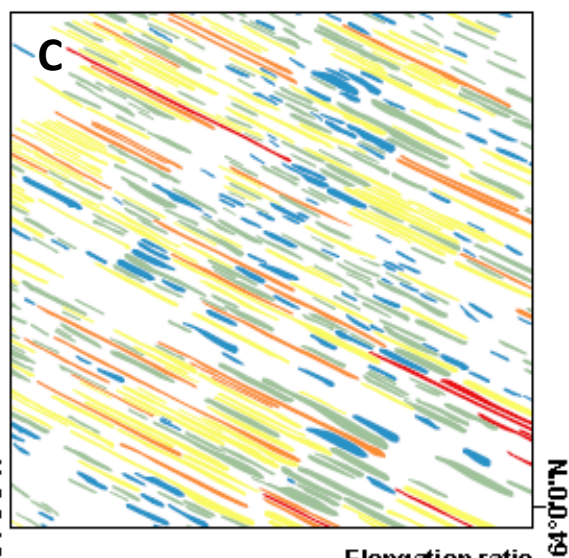
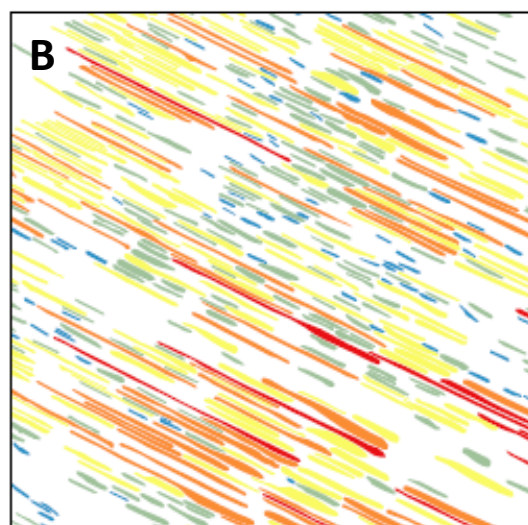
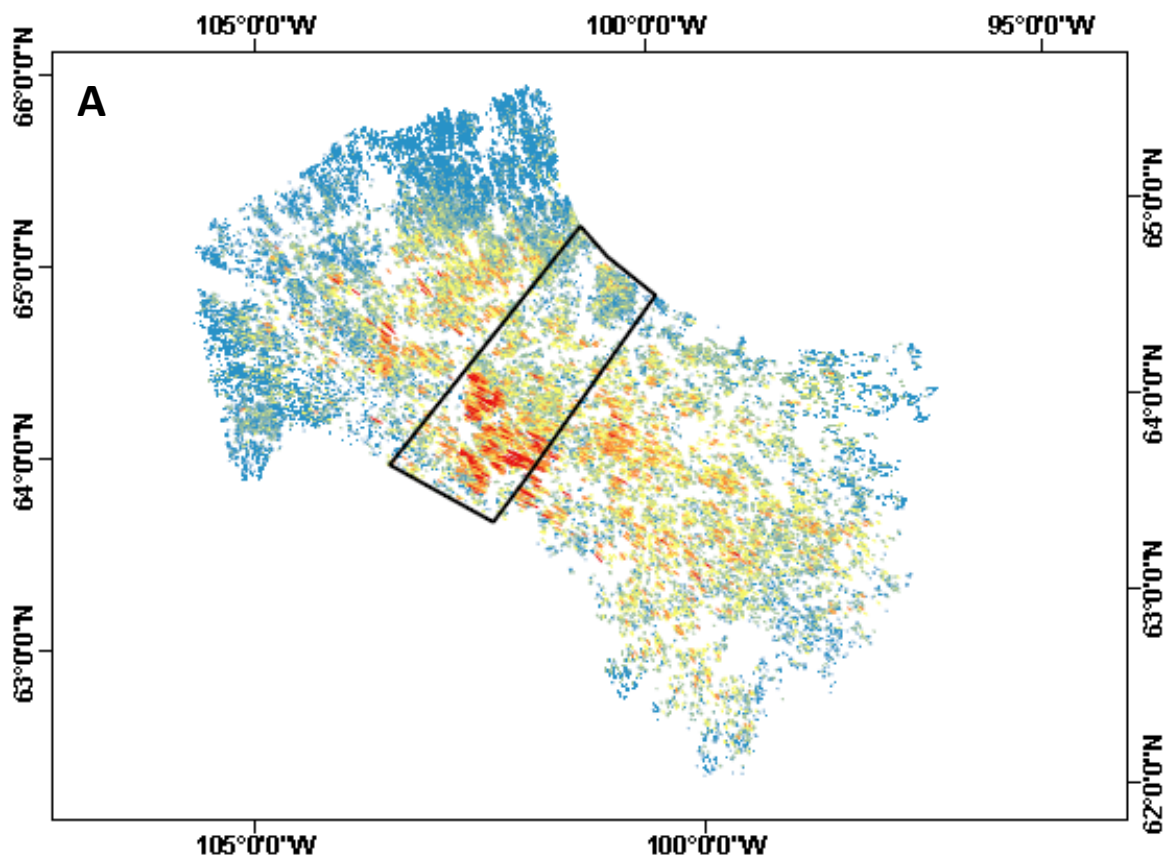


Figure 4:

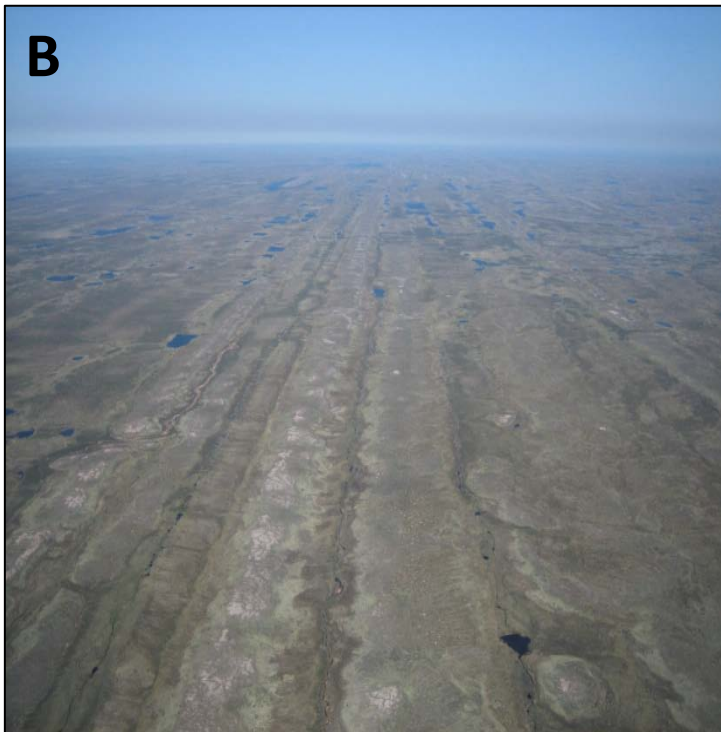
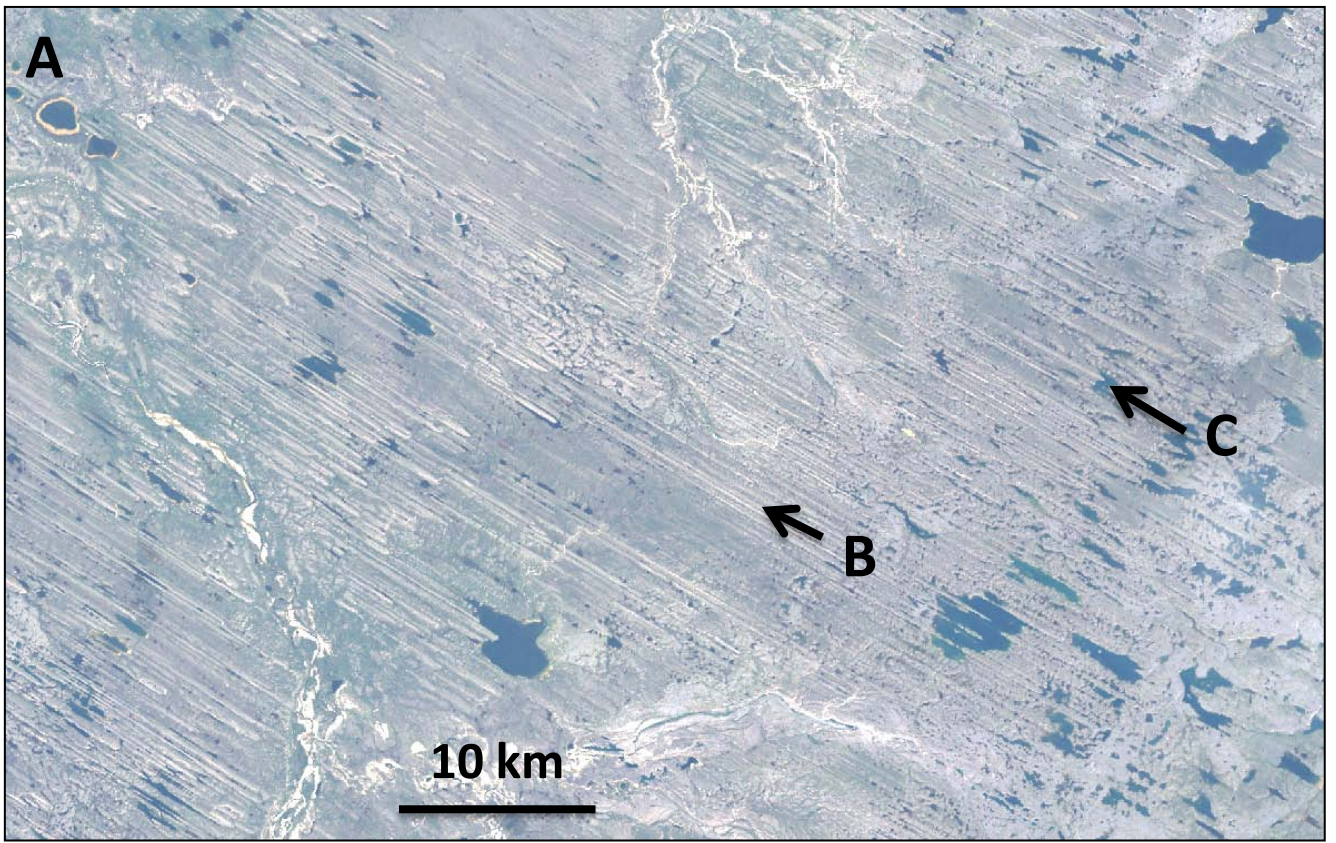


Figure 5

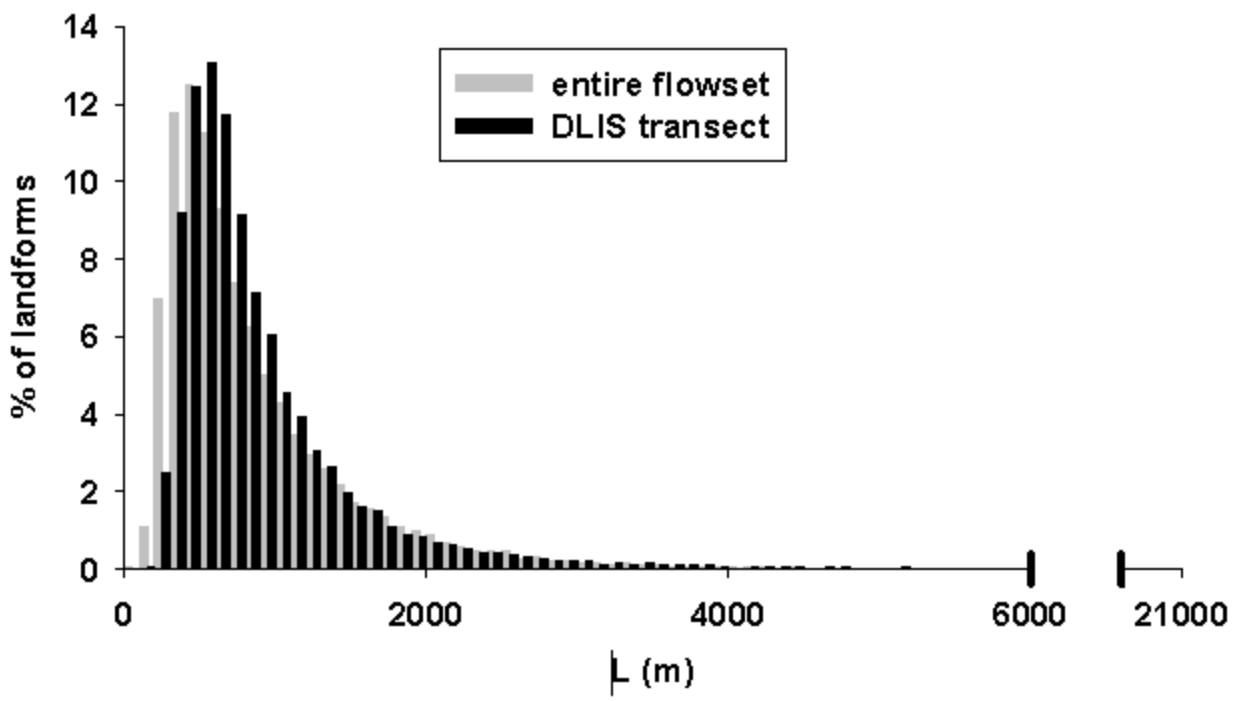


Figure 6:

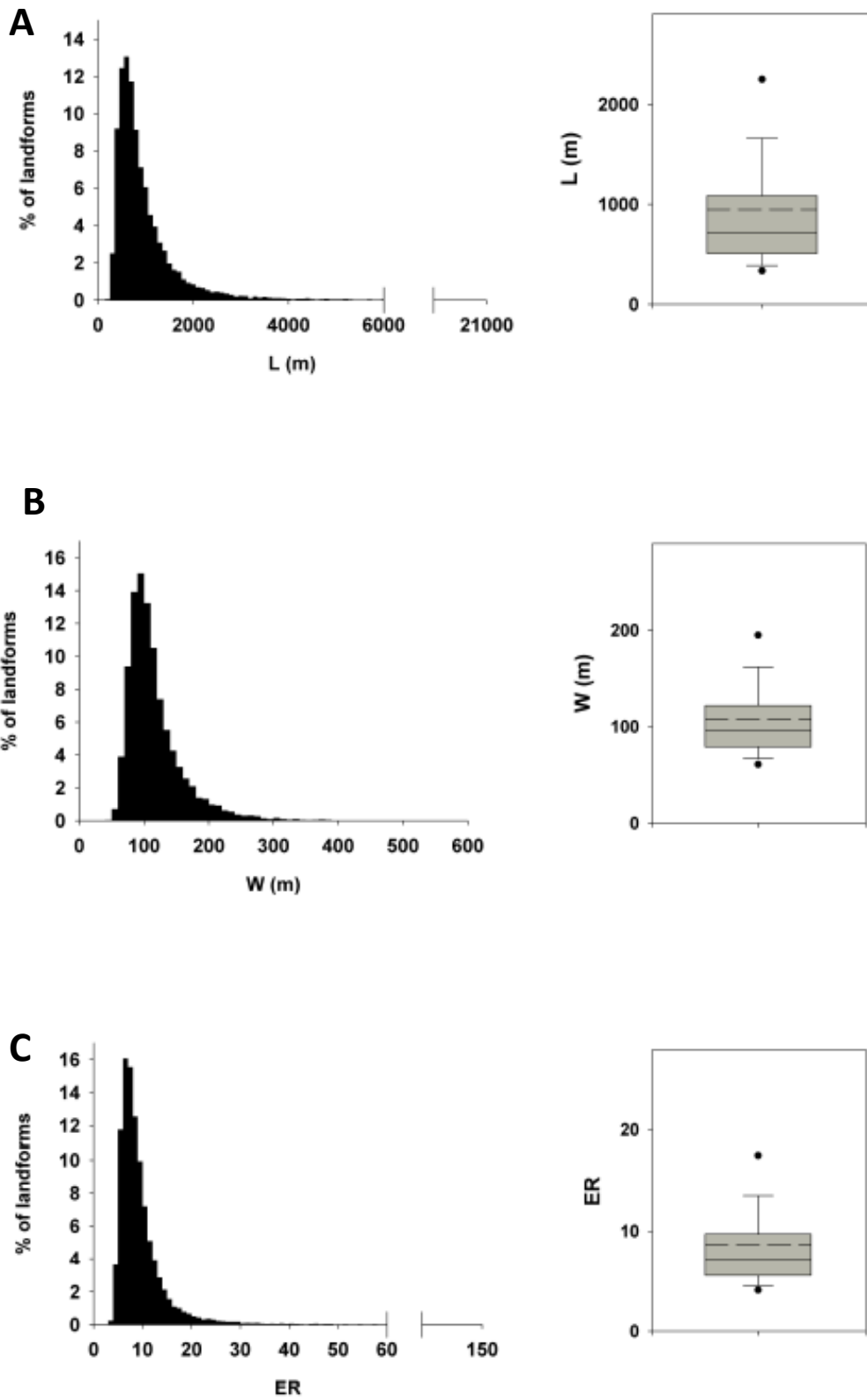


Figure 7

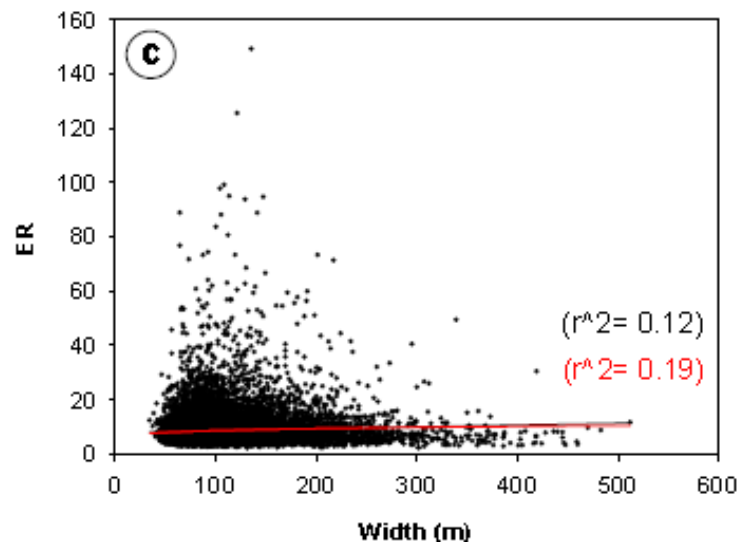
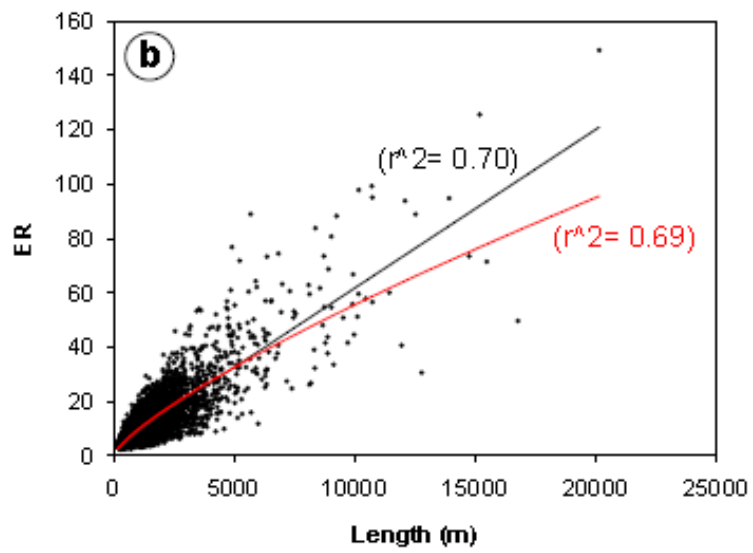
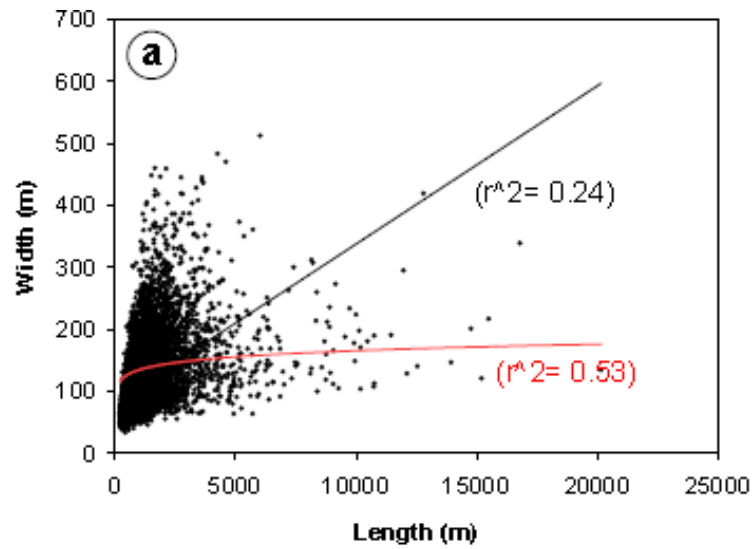


Figure 8

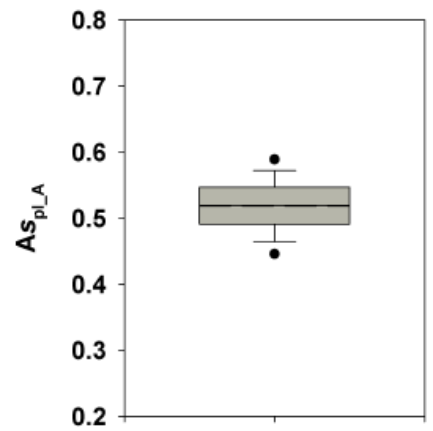
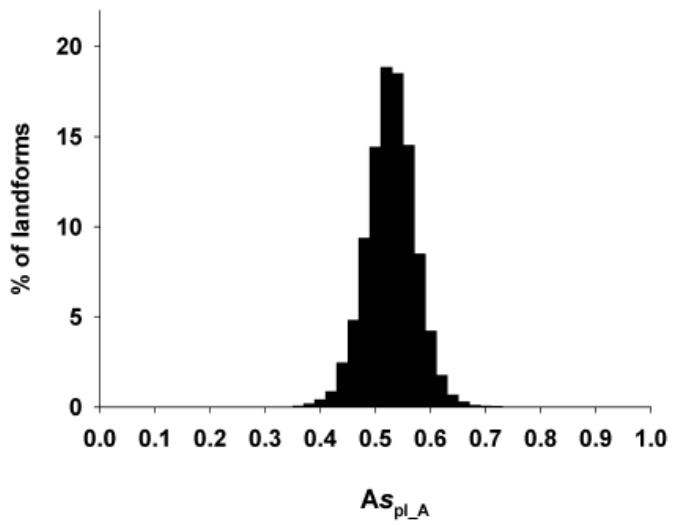


Figure 9

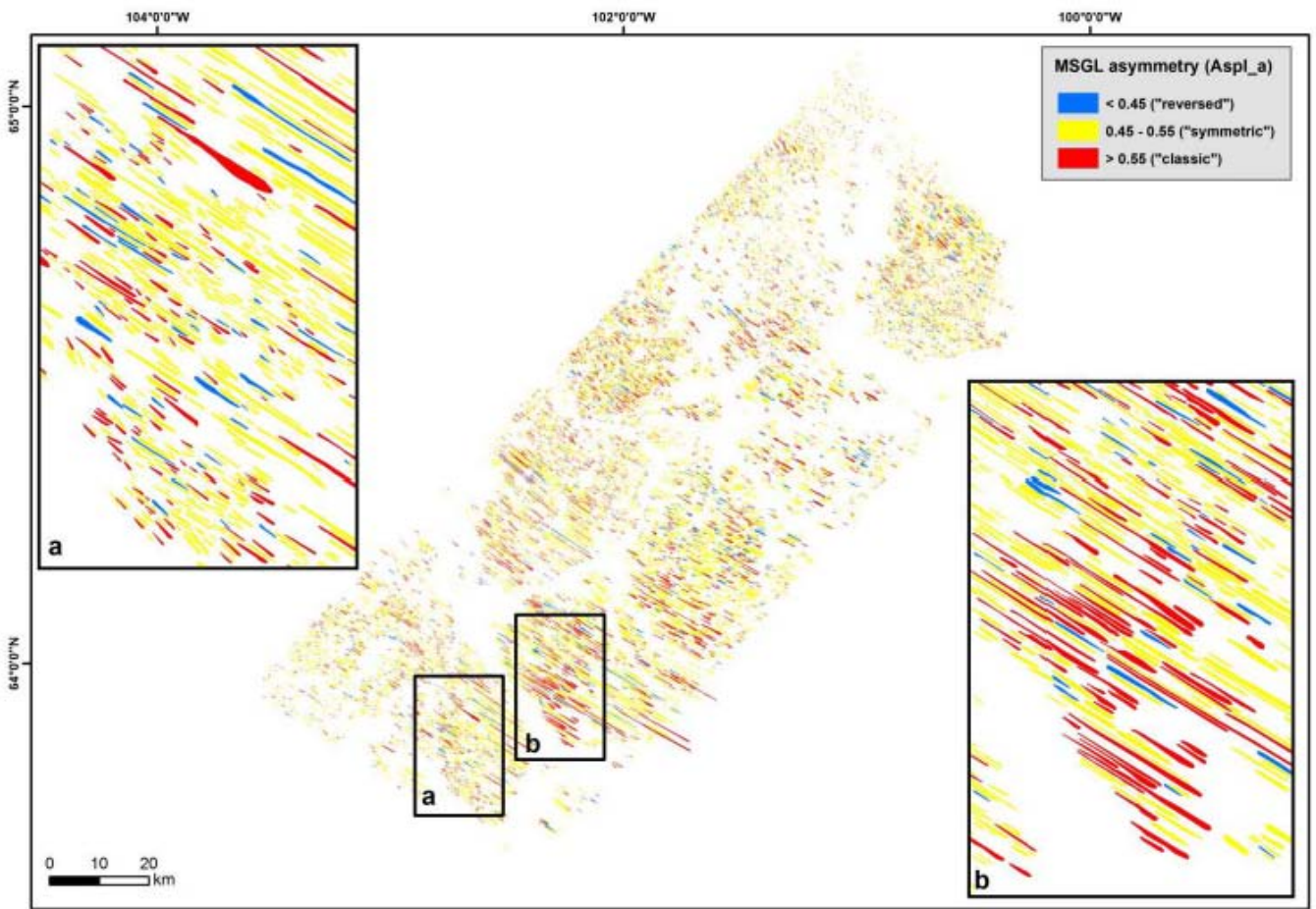


Figure 10

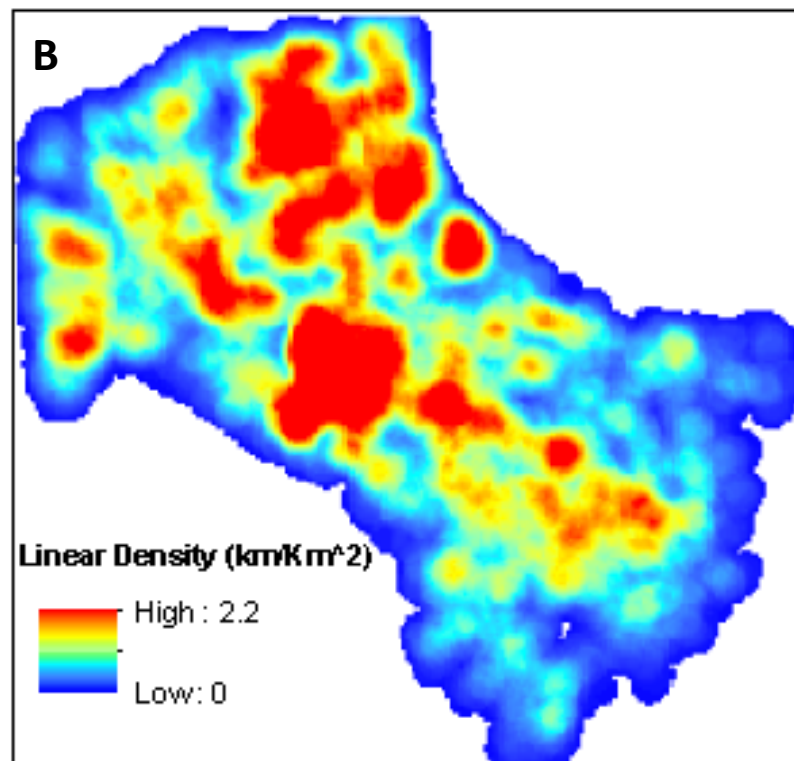
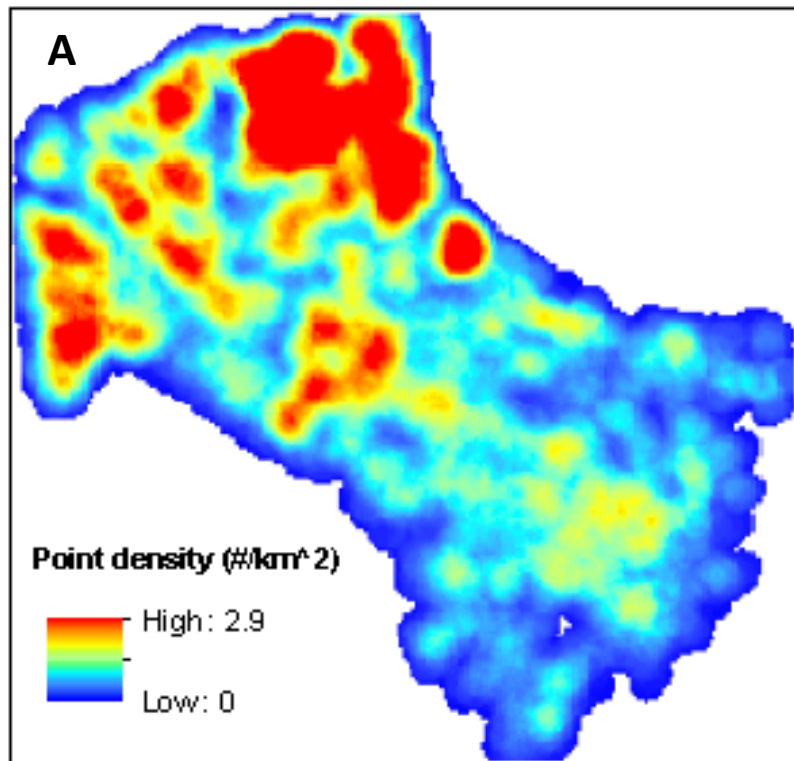


Figure 11

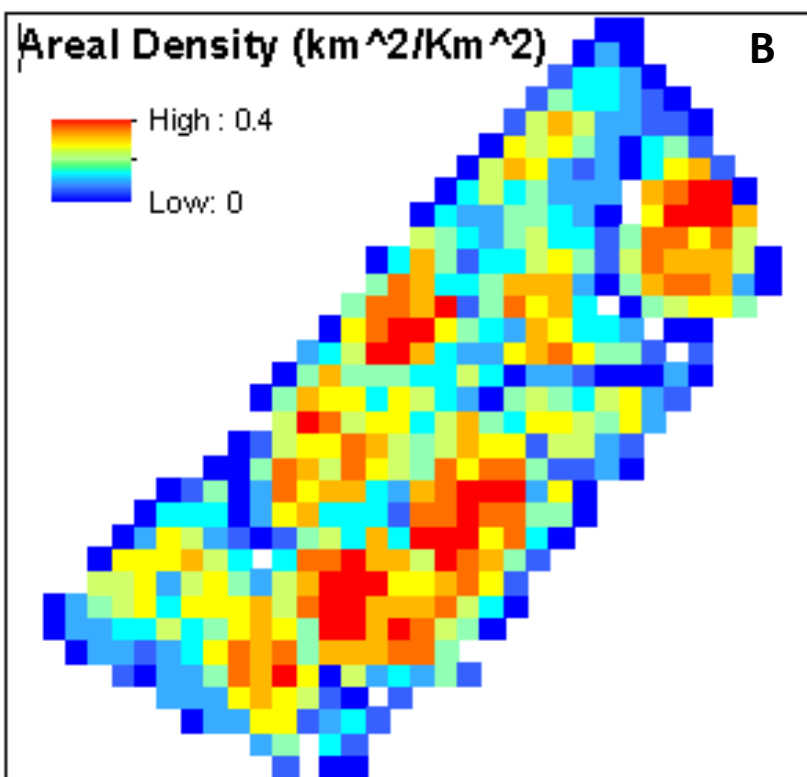
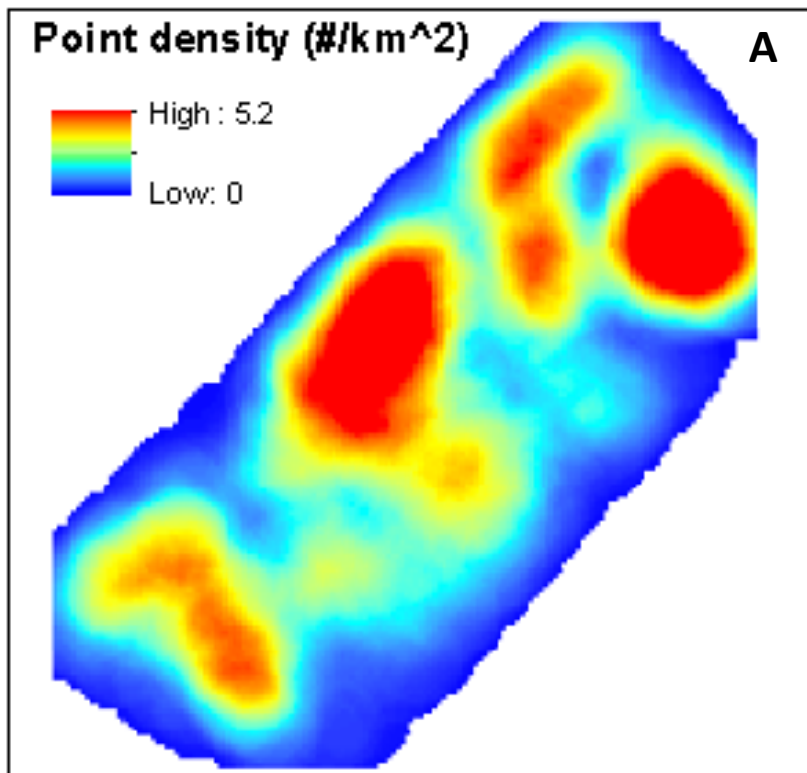
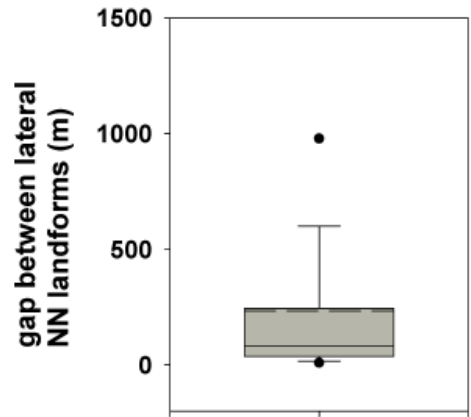
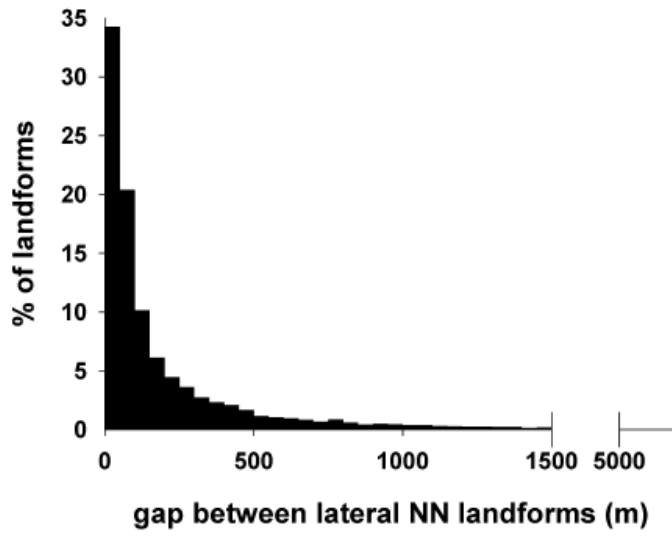
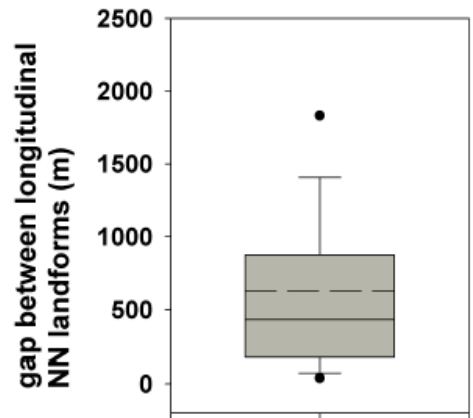
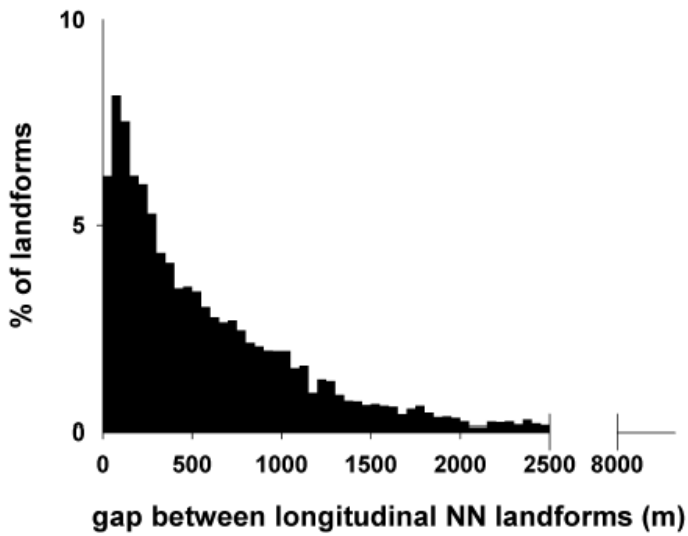
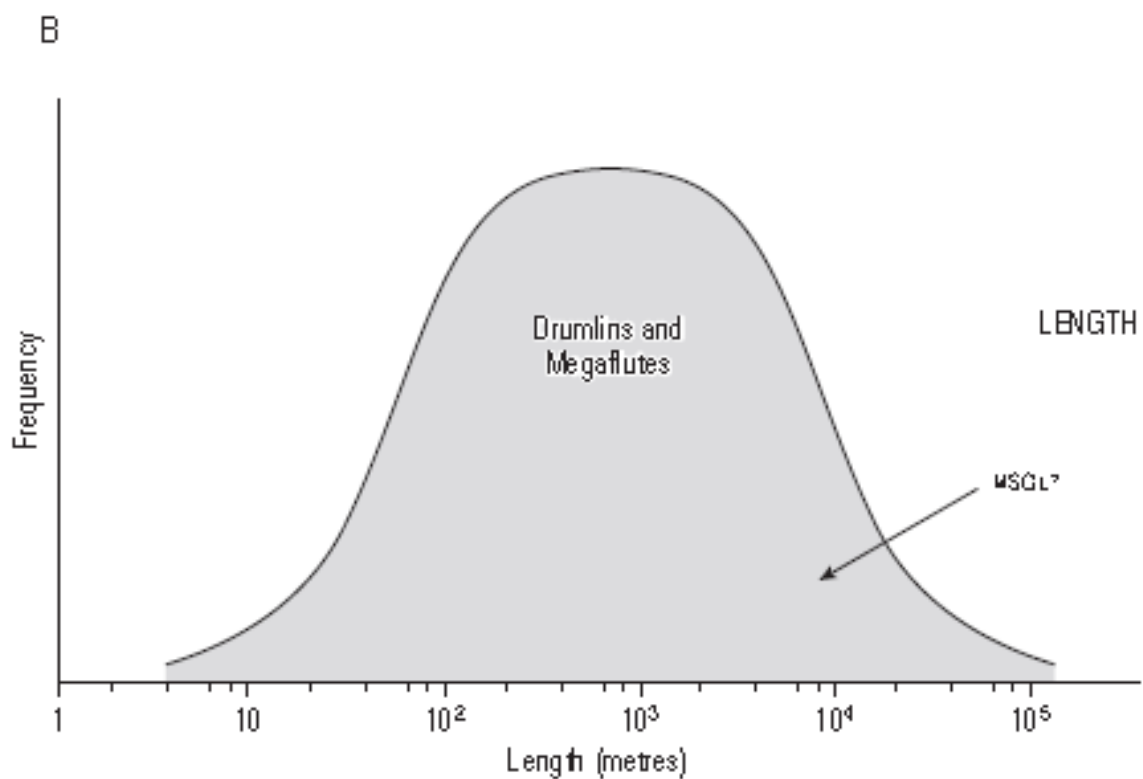
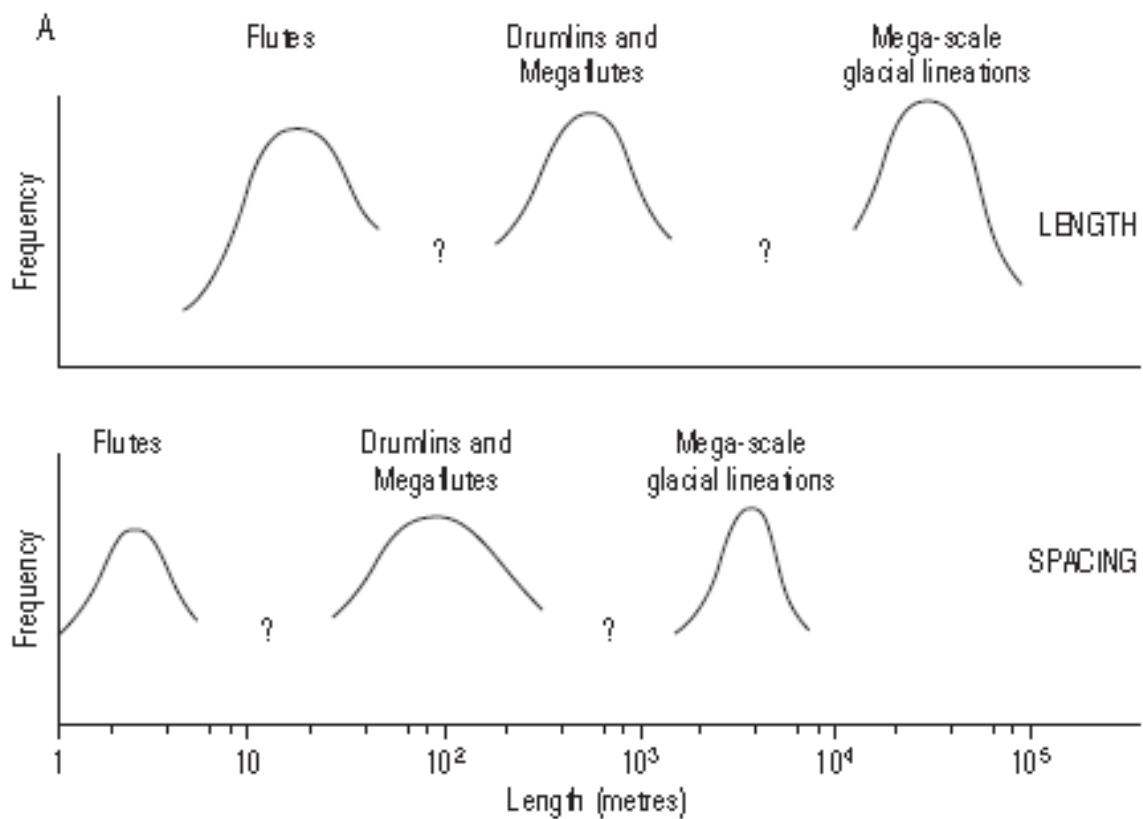


Figure 12

**A****B****Figure 13:**



**Figure 14**

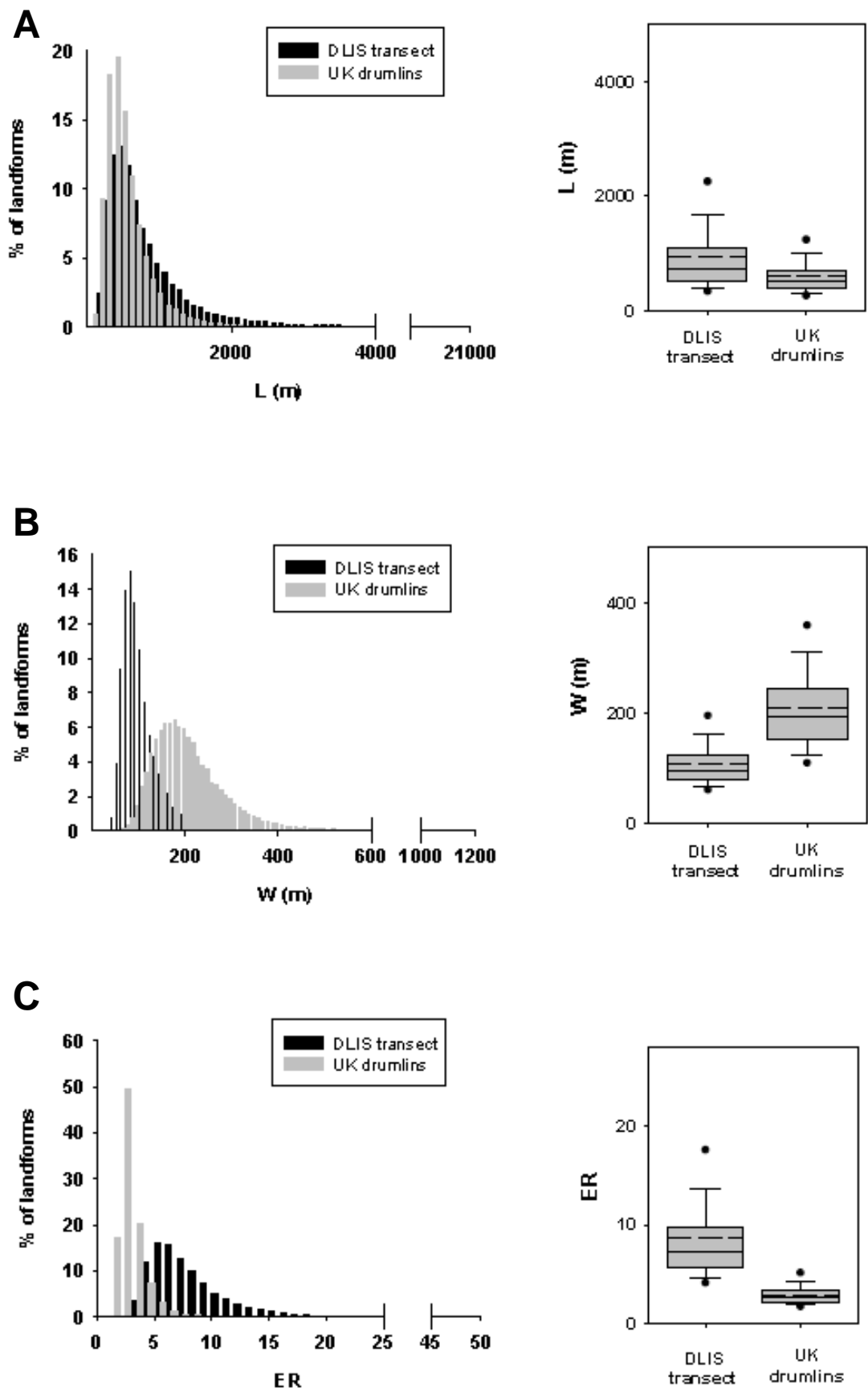


Figure 15

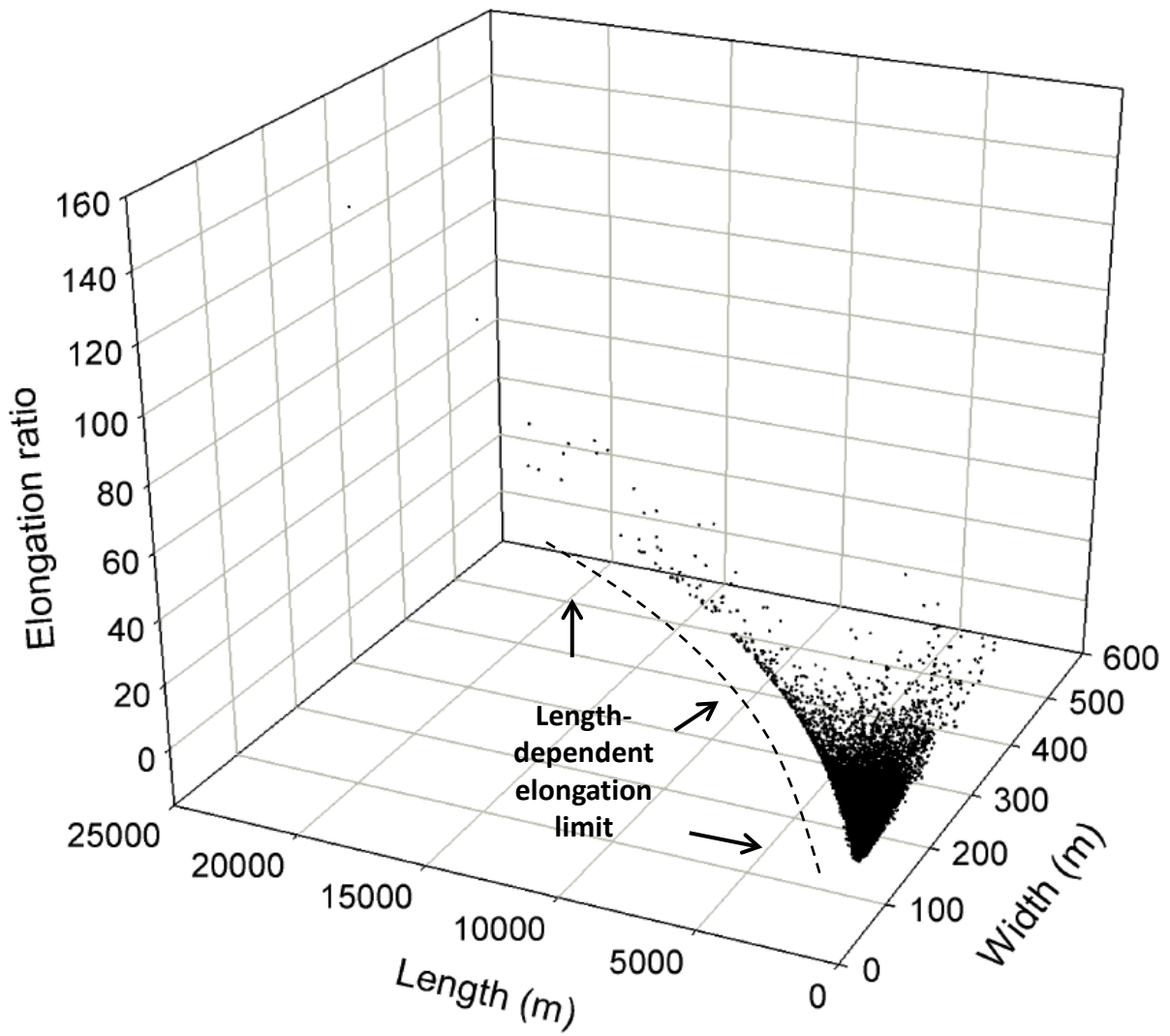


Figure 16

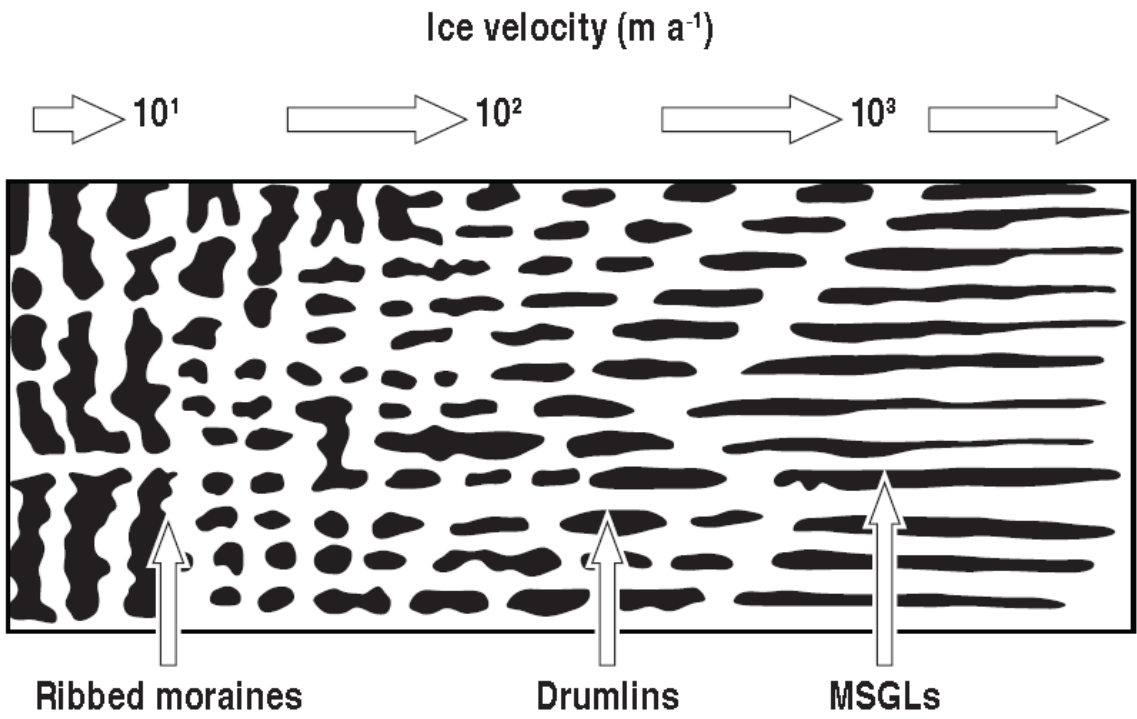


Figure 17